

# Dietary fiber guar gum-induced shift in gut microbiota metabolism and intestinal immune activity enhances susceptibility to colonic inflammation

Devendra Paudel<sup>a</sup>, Divek V. T. Nair<sup>a</sup>, Sangshan Tian<sup>a</sup>, Fuhua Hao<sup>b</sup>, Umesh K. Goand<sup>a</sup>, Grace Joseph<sup>a</sup>, Eleni Prodes<sup>a</sup>, Zhi Chai<sup>c</sup>, Chloé E.M. Robert<sup>d,e</sup>, Benoit Chassaing<sup>d,e</sup>, Andrew D. Patterson<sup>b</sup>, and Vishal Singh <sup>a</sup>

<sup>a</sup>Department of Nutritional Sciences, The Pennsylvania State University, University Park, PA, USA; <sup>b</sup>Department of Veterinary and Biomedical Sciences, The Pennsylvania State University, University Park, PA, USA; <sup>c</sup>Department of Genetics and Genomic Sciences, Icahn School of Medicine at Mount Sinai, New York, NY, USA; <sup>d</sup>INSERM U1016, team “Mucosal microbiota in chronic inflammatory diseases”, CNRS UMR 8104, Université Paris Cité, Paris, France; <sup>e</sup>INSERM U1306, Microbiome-Host Interaction group, Institut Pasteur, Université Paris Cité, Paris, France

## ABSTRACT

With an increasing interest in dietary fibers (DFs) to promote intestinal health and the growth of beneficial gut bacteria, there is a continued rise in the incorporation of refined DFs in processed foods. It is still unclear how refined fibers, such as guar gum, affect the gut microbiota activity and pathogenesis of inflammatory bowel disease (IBD). Our study elucidated the effect and underlying mechanisms of guar gum, a fermentable DF (FDF) commonly present in a wide range of processed foods, on colitis development. We report that guar gum containing diet (GuD) increased the susceptibility to colonic inflammation. Specifically, GuD-fed group exhibited severe colitis upon dextran sulfate sodium (DSS) administration, as evidenced by reduced body weight, diarrhea, rectal bleeding, and shortening of colon length compared to cellulose-fed control mice. Elevated levels of pro-inflammatory markers in both serum [serum amyloid A (SAA), lipocalin 2 (Lcn2)] and colon (Lcn2) and extensive disruption of colonic architecture further affirmed that GuD-fed group exhibited more severe colitis than control group upon DSS intervention. Amelioration of colitis in GuD-fed group pre-treated with antibiotics suggest a vital role of intestinal microbiota in GuD-mediated exacerbation of intestinal inflammation. Gut microbiota composition and metabolite analysis in fecal and cecal contents, respectively, revealed that guar gum primarily enriches Actinobacteriota, specifically *Bifidobacterium*. Guar gum also altered multiple genera belonging to phyla Bacteroidota and Firmicutes. Such shift in gut microbiota composition favored luminal accumulation of intermediary metabolites succinate and lactate in the GuD-fed mice. Colonic IL-18 and tight junction markers were also decreased in the GuD-fed group. Importantly, GuD-fed mice pre-treated with recombinant IL-18 displayed attenuated colitis. Collectively, unfavorable changes in gut microbiota activity leading to luminal accumulation of lactate and succinate, reduced colonic IL-18, and compromised gut barrier function following guar gum feeding contributed to increased colitis susceptibility.

## SUMMARY

- Guar gum increased susceptibility to colitis
- Guar gum-induced exacerbation of colitis is gut microbiota dependent
- Guar gum-induced shift in microbiota composition favored the accumulation of luminal intermediate metabolites succinate and lactate
- Guar gum-fed mice exhibited reduced colonic level of IL-18 and tight junction molecules.
- Exogenous IL-18 administration partly rescued mice from guar gum-induced colitis susceptibility

## ARTICLE HISTORY

Received 22 August 2023  
Revised 20 March 2024  
Accepted 4 April 2024



## KEYWORDS


Added fiber; dysbiosis; inflammatory bowel disease; succinate; lactate; *Bifidobacterium*; interleukin-18 (IL-18)

## Introduction

Guar gum is a soluble dietary fiber that is extracted from the seeds of *Cyamopsis tetragonoloba* L., commonly known as guar or cluster bean. Guar gum is frequently used in commercially formulated food

products, including ice cream, yogurt, processed cheeses, bakery products, salad dressings, and beverages.<sup>1</sup> Food based industrial applications of guar gum are mainly attributable to its ability to form hydrogen bonding, with water molecules

**CONTACT** Vishal Singh  [vxs28@psu.edu](mailto:vxs28@psu.edu)  Department of Nutritional Sciences, The Pennsylvania State University, 110 Chandlee Bldg, University Park, PA 16802, USA

 Supplemental data for this article can be accessed online at <https://doi.org/10.1080/19490976.2024.2341457>

© 2024 The Author(s). Published with license by Taylor & Francis Group, LLC.

This is an Open Access article distributed under the terms of the Creative Commons Attribution-NonCommercial License (<http://creativecommons.org/licenses/by-nc/4.0/>), which permits unrestricted non-commercial use, distribution, and reproduction in any medium, provided the original work is properly cited. The terms on which this article has been published allow the posting of the Accepted Manuscript in a repository by the author(s) or with their consent.

resulting in its use as stabilizer, and thickener in various food products.<sup>1</sup> Moreover, guar gum is also used as an emulsifier, as it can prevent oil droplets from coalescing. Several clinical and pre-clinical studies suggest that in the healthy gut, guar gum induces a favorable shift in the composition of the gut microbiota and enriches SCFA-producing bacteria.<sup>2–5</sup> Nonetheless, the effect of guar gum on the intestinal health under an inflammatory context, such as during Inflammatory bowel disease (IBD), remains unclear.

IBD, including Crohn's Disease (CD) and Ulcerative Colitis (UC), is characterized by an adverse immune response resulting in inflammation of the gastrointestinal tract accompanied by a disturbance of the gut microbiota composition and activity. While the underlying mechanisms of IBD are not fully understood, a combination of genetic predisposition and environmental triggers, including atypical gut microbiota activity that disrupts intestinal immune homeostasis,<sup>6,7</sup> largely contribute to the initiation and progression of the disease. Accordingly, individuals with IBD tend to have a microbiome characterized by decreased diversity and distinct metabolic activity.<sup>8,9</sup> Key metabolites produced by the gut microbiota including short-chain fatty acids (SCFAs), branched-chain amino acids (BCAAs), and succinate, may play a role in the regulation of intestinal inflammation during IBD. SCFAs include propionate, acetate, and butyrate, and are primarily produced by the bacterial fermentation of fermentable dietary fibers (FDFs). In the colonic epithelium, SCFAs act as a primary energy source and regulate the intestinal immune responses.<sup>10</sup> Specific amino acids, including BCAAs (valine, leucine, and isoleucine), are found in higher concentrations in patients with CD,<sup>11</sup> and diets rich in protein or amino acids have been shown to exacerbate experimental colitis.<sup>11,12</sup> Succinate, an intermediate product of the tricarboxylic acid (TCA) cycle and metabolite produced by gut microbiota, has been shown to be elevated in human and mouse models of IBD.<sup>13</sup> Elevated succinate is considered an inflammatory signal<sup>13,14</sup> and promotes intestinal inflammation.<sup>14–17</sup> Moreover, CD patients exhibit increased intestinal expression of succinate receptor (SUCNR1),<sup>15</sup> and mice lacking *Sucnr1* are protected against both intestinal inflammation and

fibrosis.<sup>15</sup> Collectively, in addition to an atypical shift in gut microbiota composition an alteration in the production of diet-derived microbial metabolites is among the primary ways by which the gut microbiota influences the progression of colonic inflammation.

Interleukin-18 (IL-18) is an IL-1 family cytokine constitutively expressed in intestinal epithelial cells (IECs). Under homeostatic conditions, IECs represent the major source of IL-18,<sup>18</sup> regulating the intestinal immune response,<sup>18</sup> and providing defense against mucosal pathogens.<sup>19,20</sup> Colonic IL-18 production is partly regulated by the commensal microbiota and dietary factors. *Prevotella* species (*Prevotella intestinalis* nov. sp.) colonization-induced shifts in microbial composition and metabolism have been shown to decrease colonic IL-18.<sup>21</sup> Taurine, an amino acid naturally occurring in protein-rich foods, has been shown to induce IL-18 secretion in colonic explants by activating the NOD-like receptor (NLR) family member NLRP6 inflammasome.<sup>22</sup> Experimental findings showed that IL-18 plays a two-sided role in the progression of colitis.<sup>23</sup> Nowarski R et al. demonstrated that mice lacking IL-18 or its receptor (IL-18r1) in intestinal epithelial cells were protected from colitis.<sup>24</sup> Whereas Iljazovic A et al. reported that diminished colonic IL-18 production before induction of colitis exacerbate intestinal inflammation, and supplementation of IL-18 did reduce the intestinal inflammation.<sup>21</sup> These differential effects may be due to the timing of the disease with IL-18 being found to have anti-inflammatory effects in early stages and pro-inflammatory effects in later stages of IBD. IL-18 has been shown to improve the severity of DSS-induced colitis and is found to have a regenerative effect on the epithelium, possibly by upregulating the production of IL-22, which is involved in epithelial repair.<sup>21,23</sup> The ubiquitous production of IL-18 by colonic epithelial cells under normal conditions and its multifaceted role in preserving gut barrier integrity and regulating immune responses led us to explore the role of colonic IL-18 in guar gum-induced colitis susceptibility.

Incorporation of refined FDFs such as guar gum in processed foods is actively promoted to enhance the diet quality based on the evidence that adequate intakes of plant-based dietary fibers are beneficial

for gastrointestinal (GI) health. However, our understanding of whether isolated FDFs are equally beneficial to their natural counterparts present in whole foods is minimal. The objective of this study was to understand the impact of isolated guar gum on the gut microbiota composition and intestinal inflammation development. While guar gum has a beneficial effect on healthy individuals, this benefit has not yet been proven in individuals with IBD. We report that guar gum-induced atypical shifts in gut microbiota composition cause an accumulation of intermediate metabolites (lactate and succinate), suppress colonic IL-18 production, and predispose mice to colonic inflammation.

## Results

### *Guar gum enhances susceptibility to colonic inflammation*

To determine the effect of guar gum on colonic inflammation, C57BL/6 wild type (WT) mice were fed either cellulose (10% w/w, control) or guar-gum (7.5% guar gum plus 2.5% w/w cellulose) containing diet (GuD; [Table 1](#)) for 4 weeks followed by dextran sulfate sodium (DSS) containing water for 1 week. Commonly, DSS is administered

in a range of doses from 2.5% w/v to 3% w/v to induce colitis in C57BL/6 WT mice.<sup>25,26</sup> Therefore, after 4 weeks, mice were switched to drinking water containing 2.8% w/v of DSS. Unexpectedly, both the control and GuD-fed group displayed a loss in body weight (wt.) and rectal bleeding starting from day 4. A significant number of GuD-fed mice receiving 2.8% DSS died on day 7 (50%; 3 out of 6 mice, survival curve is not shown). This high mortality rate prompted us to conduct another experiment with a similar design (2.8% DSS) but terminated it earlier, on day 6 ([Figure S1a](#)). Even 6-day-post DSS administration, the GuD-fed group had significant body weight loss ( $\geq 20\%$  of initial body wt.) ([Figure S1b](#)). Notably, relative to the control group, early (day 4) and rapid loss of body wt., extensive rectal bleeding, and high serum lipocalin 2 (Lcn2), and mortality were observed in GuD-fed mice ([Figure S1b-i](#)), indicating that guar gum worsened the DSS-induced colitis. Off note, the one-hour fecal output determination, performed in triplicates at week 4 before DSS intervention, showed no significant difference between the Con and GuD-fed groups ([Figure S2](#)). This indicates that intestinal transit time<sup>27</sup> is comparable between these two groups. To further examine whether feeding mice with

**Table 1.** Control and guar gum diet composition.

Diet Formulas Product #	Cellulose containing diet (Con)		Guar gum containing diet (GuD)	
	D12081402		D12081409	
	gm%	kcal%	gm%	kcal%
Protein	18.5	20	19.0	20
Carbohydrate	61.8	65	60.8	63
Fat	6.4	15	6.5	15
Total		100		100
kcal/gm	3.78		3.88	
Ingredient	gm	kcal	gm	kcal
Casein	200	800	200	800
L-Cystine	3	12	3	12
Corn Starch	409	1636	381	1524
Maltodextrin 10	110	440	110	440
Dextrose	150	600	150	600
Cellulose, BW200	100	0	25	0
Guar Gum	0	0	75	112.5
Agar Agar 100	0	0	0	0
Lard	0	0	0	0
Soybean Oil	70	630	70	630
Mineral Mix S10026	10	0	10	0
Dicalcium Phosphate	13	0	13	0
Calcium Carbonate	5.5	0	5.5	0
Potassium Citrate, 1 H <sub>2</sub> O	16.5	0	16.5	0
Vitamin Mix V10001	10	40	10	40
Choline Bitartrate	2	0	2	0
Yellow Dye #5, FD&C	0	0	0.025	0
Red Dye #40, FD&C	0	0	0	0
Blue Dye #1, FD&C	0.05	0	0.025	0

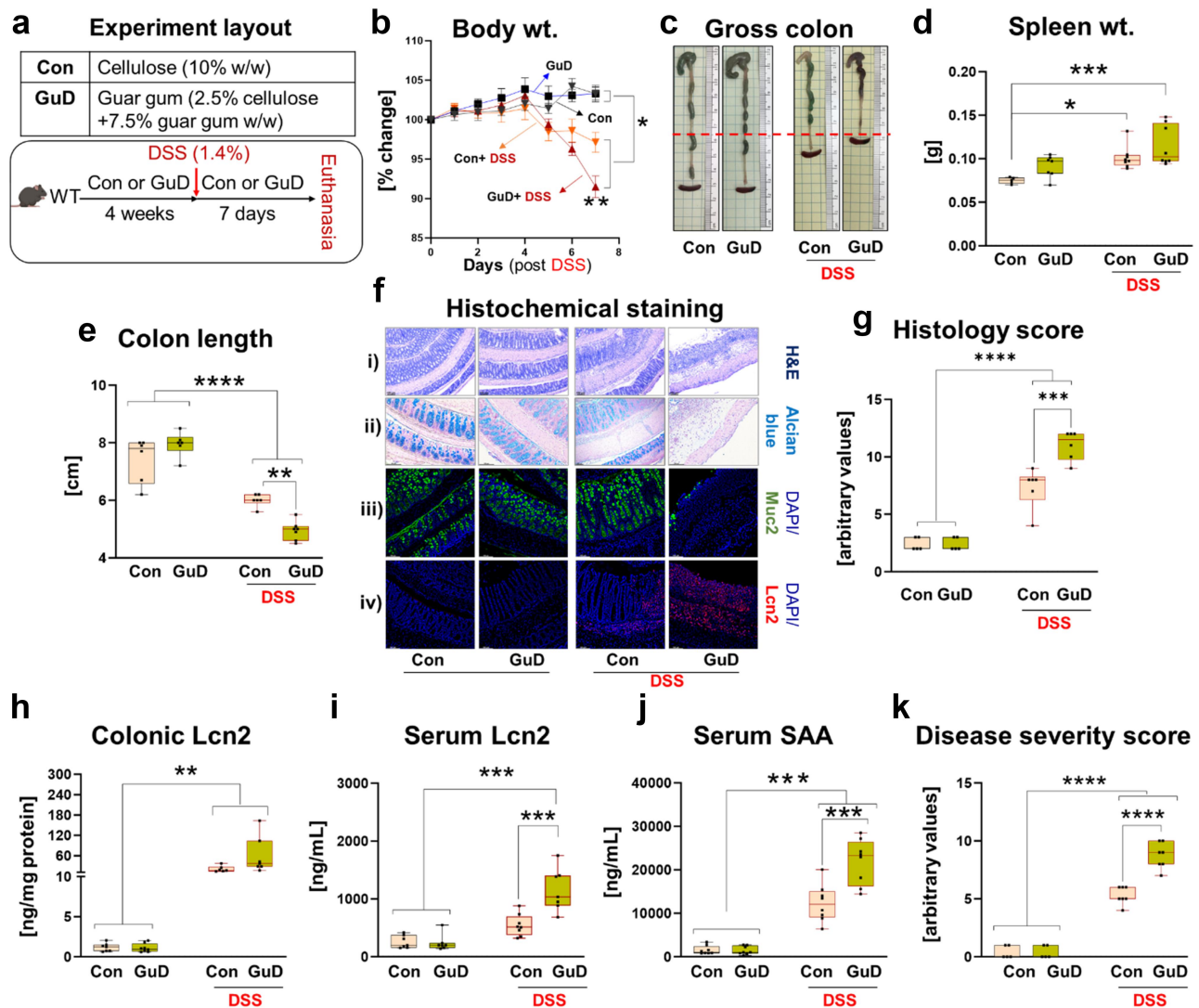


**Figure 1.** Guar gum exacerbated DSS-induced acute colitis. (a) Experimental design employed to investigate the effect of guar gum (GuD) on acute colitis. Four weeks old WT mice ( $n=6-7$  per group) were maintained on control (Con) or GuD for 4-weeks before colitis was induced by switching to DSS (1.4% w/v) containing water for 7 days. (b) Percent change in body weight. (c) Gross colon appearance (d) Spleen weight. (e) Colon length. (f i-iv) Representative images of: H&E (i) and alcian blue (ii)-stained colon sections (original magnification,  $\times 100$ ). (iii-iv) Colonic sections displaying immunohistochemical staining for mucin 2 (Muc2) (iii, green), and Lcn2 (iv, red). DAPI was used to visualize nucleus [blue, (original magnification,  $\times 200$ )]. (g) Histopathological scores from blinded evaluation of H&E-stained colonic sections. (h-j) Colonic and Serum Lcn2 and SAA. (k) Disease severity was assessed by summing scores (0–4) for weight loss, stool consistency, fecal occult blood, and histopathological changes. Values are presented as mean  $\pm$  SEM. (d–e and g–k) One-way ANOVA, multiple comparisons test. \* $p < .05$ , \*\* $p < .01$ , \*\*\* $p < .001$ , and \*\*\*\* $p < .0001$ .

GuD increases susceptibility to colonic inflammation, we next instigated colitis with lower DSS concentration (1.4%) than previously used (Figure 1(a)). Likewise, at reduced dose, the GuD-fed group exhibited significant loss of body weight and decreased colon length compared to the control group (Figure 1(b,c,e)). DSS-treated GuD-fed mice displayed increasing trend in spleen weight albeit with high variability when compared to DSS treated control group (Figure 1(d)). Furthermore,

histological analysis revealed relatively more disruption of crypt structure and extensive immune cell infiltration in mucosa and submucosa in GuD-fed group (Figure 1(f,g)) affirmed that guar gum increased susceptibility to colitis. Moreover, DSS-treated GuD-fed mice displayed substantial reduction in colonic mucin, as evidenced by reduced Alcian blue-stained area and mucin 2 immunostaining (Figure 1(fii-iii)). Immunohistochemical staining revealed higher colonic Lcn2 expression



(Figure 1(fiv)) in the GuD-fed group compared to the DSS-treated control group. However, ELISA-based measurement of colonic Lcn2 in the proximal region showed an upward trend (Figure 1(h)), but this difference did not reach statistical significance, likely due to higher variability observed within the GuD-fed group in the proximal colon. Notably, relative to DSS-treated controls, GuD-fed mice showed a significant elevation of systemic Lcn2 and serum amyloid A (SAA) (Figure 1(i,j)). Consistent with these observations, the GuD-fed group displayed increased colitis severity scores (Figure 1(k)). At basal level, no marked difference in the markers of colonic inflammation was observed between control and GuD-fed mice (Figure 1). Altogether, these results demonstrated that GuD worsened colonic inflammation and mucosal damage triggered by epithelial injury.

#### ***Gut microbiota mediates exacerbation of colitis in guar gum-fed mice***

Alterations in microbiota composition and metabolism have been shown to regulate the susceptibility to colitis.<sup>28,29</sup> Specifically, environmental factors, such as Western diet and antibiotic exposure, induce an imbalance in microbiota composition that promotes colitis development.<sup>30,31</sup> Hence, we next hypothesized that a GuD-induced shift in gut microbiota composition and activity predisposed GuD-fed mice to colitis. To test the contributory role of gut microbiota, we ablated microbial communities residing in the gut by administering a cocktail of antibiotics and antifungal agent (Abx) via drinking water. Both Abx and untreated mice maintained on GuD or control diet for three weeks were switched to DSS-containing water for seven days (Figure 2(a)). The Abx mixture water was discontinued during the DSS-intervention period. To our surprise, Abx intervention failed to protect from DSS-induced colitis in the control group (Figure 2(b–k)). Notably, microbiota depletion ameliorated colitis in GuD-fed mice, as evidenced by improved body weight recovery, reduced spleen weight, and increased colon length than the DSS only group (Figure 2(b–e)). H&E and Alcian blue staining, along with Muc2 and Lcn2 immunostaining, revealed considerably less crypt disruption, increased goblet cells, enhanced mucin production,

and reduced Lcn2 expression compared to the DSS-treated control group (Figure 2(f,g)). Consistent with these observations, colonic and serum Lcn2 levels, as well as serum SAA, were significantly decreased in the Abx group (Figure 2(h–j)). Importantly, Abx intervention resulted in a reduced overall disease severity score in the DSS-treated GuD-fed group (Figure 2(k)). These results demonstrated that gut microbiota plays a role in exacerbating susceptibility to guar gum-mediated colitis.

#### ***Guar gum alters gut microbiota composition, enriching Actinobacteriota***

Fermentable dietary fibers are among the chief modulators of the composition and function of gut microbiota. Intriguingly, DSS-induced colonic inflammation was ameliorated upon microbiota depletion in GuD-fed mice. Therefore, we surmised that GuD-induced shift in microbiota composition may augment susceptibility to colitis. Next, we assessed gut microbiota composition alterations after 5 weeks of guar gum or control diet feeding in mice without inflammation (Figure 3(a)). Principal Coordinate Analysis (PCoA) plot derived from 16S rRNA analysis showed differences in the fecal microbiota composition between GuD and control diet, albeit with high variability (Figure 3(b)). Moreover, Shannon diversity index analysis indicated a marginal reduction of microbiota alpha diversity in GuD-fed mice compared to control (Figure 3(c)). A detailed microbiota composition analysis, through Microbiome Multivariable Associations with Linear Models (MaAsLin2)-based statistical analysis, highlighted specific alterations in groups of bacteria belonging to phyla Actinobacteriota, Bacteroidota, and Firmicutes. More specifically, the relative abundance of Actinobacteriota phylum was substantially higher in GuD than control group (Figure 3(d)). The increased abundance of phylum Actinobacteriota in GuD-fed group was largely derived by enrichment (>40 folds) of *Bifidobacterium* (Figure 3(e)), a known producer of succinic acid.<sup>32</sup> Among the phylum Bacteroidota, GuD-fed mice showed a significant decrease in genus *Bacteroides* (Figure 3(f)), while abundance of *Alloprevotella* remained unchanged.

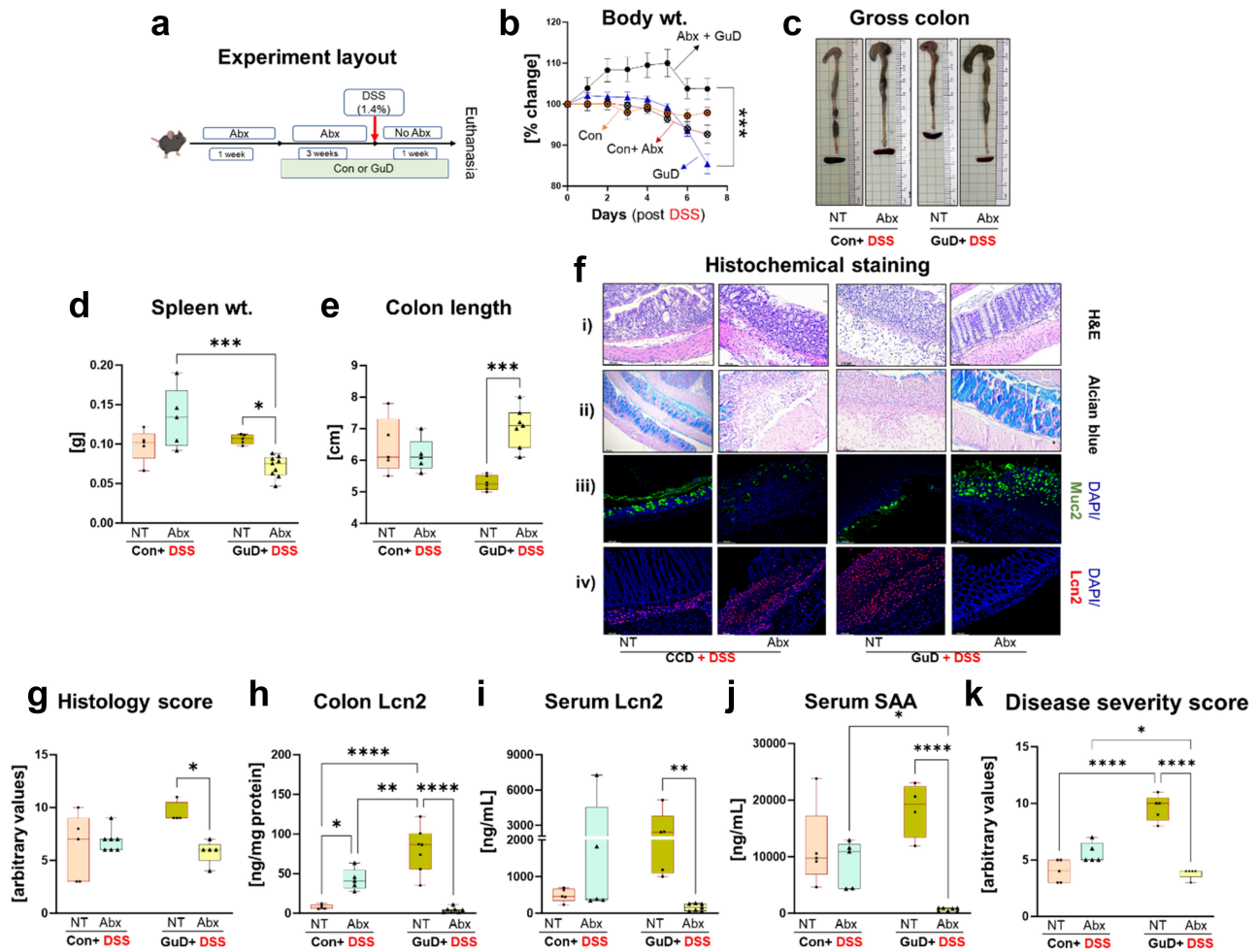


**Figure 2.** Antibiotic-mediated depletion of gut microbiota rescued GuD-fed mice from DSS-induced colitis. (a) Experimental design showing the timeline for administration of antibiotics mixture. Experimental groups received either regular (no treatment; NT) or antibiotic mixture-containing (Abx) water maintained on a Con or GuD diet and switched to DSS (1.4% w/v) during the last week. (b) Percent change in body weight. (c) Gross colon appearance. (d) Spleen weight. (e) Colon length. (f) Representative H&E and Alcian blue stained images (i-ii, original magnification,  $\times 100$ ) of colon, and sections immunostained for Muc2 (iii, green), and Lcn2 (iv, red) (original magnification,  $\times 200$ ) (g) Histopathological scores derived from blinded evaluation of H&E-stained colonic sections. (h) Colonic Lcn2. Serum (i) Lcn2 and (j) SAA. (k) Disease severity score. Data, presented as mean  $\pm$  SEM, were combined from two independent experiments. Unpaired t-test. \*  $p < .05$ , \*\*  $p < .01$ , \*\*\*  $p < .001$ , and \*\*\*\*  $p < .0001$ .

Phylum Firmicutes, often associated with the production of SCFA and BCAA, exhibited highest alterations in response to GuD intervention (Figure 3(g)). Notably, the relative abundance of *Lactobacillus*, which primarily produces lactate as the major end product of complex carbohydrate fermentation, was increased in response to GuD intervention (Figure 3(gi)). We observed, in contrast, increased abundance of *Clostridia*-UCG.014 in GuD fed mice (Figure 3(gii)) whose reduction has been found to be associated with impaired barrier function in healthy relatives of patients with CD.<sup>33</sup> The other groups within the Firmicutes phylum showed decreased abundance

in GuD-fed group than control mice, including *Lachnospiraceae* ASF356, *Harryflintia*, *Tyzzzeria*, *Romboutsia*, *Lachnoclostridium*, and *Blautia* (Figure 3(giii-viii)). Interestingly, most of the bacterial strains (listed above) reduced upon guar gum feeding displayed similar trend, reduction, in patients with UC.<sup>34–36</sup>

#### Guar gum favors the production of succinate in intestinal lumen and elevates the colonic expression of succinate receptor

Dietary fibers are a primary substrate for microbial fermentation, and the fiber fermentation-derived

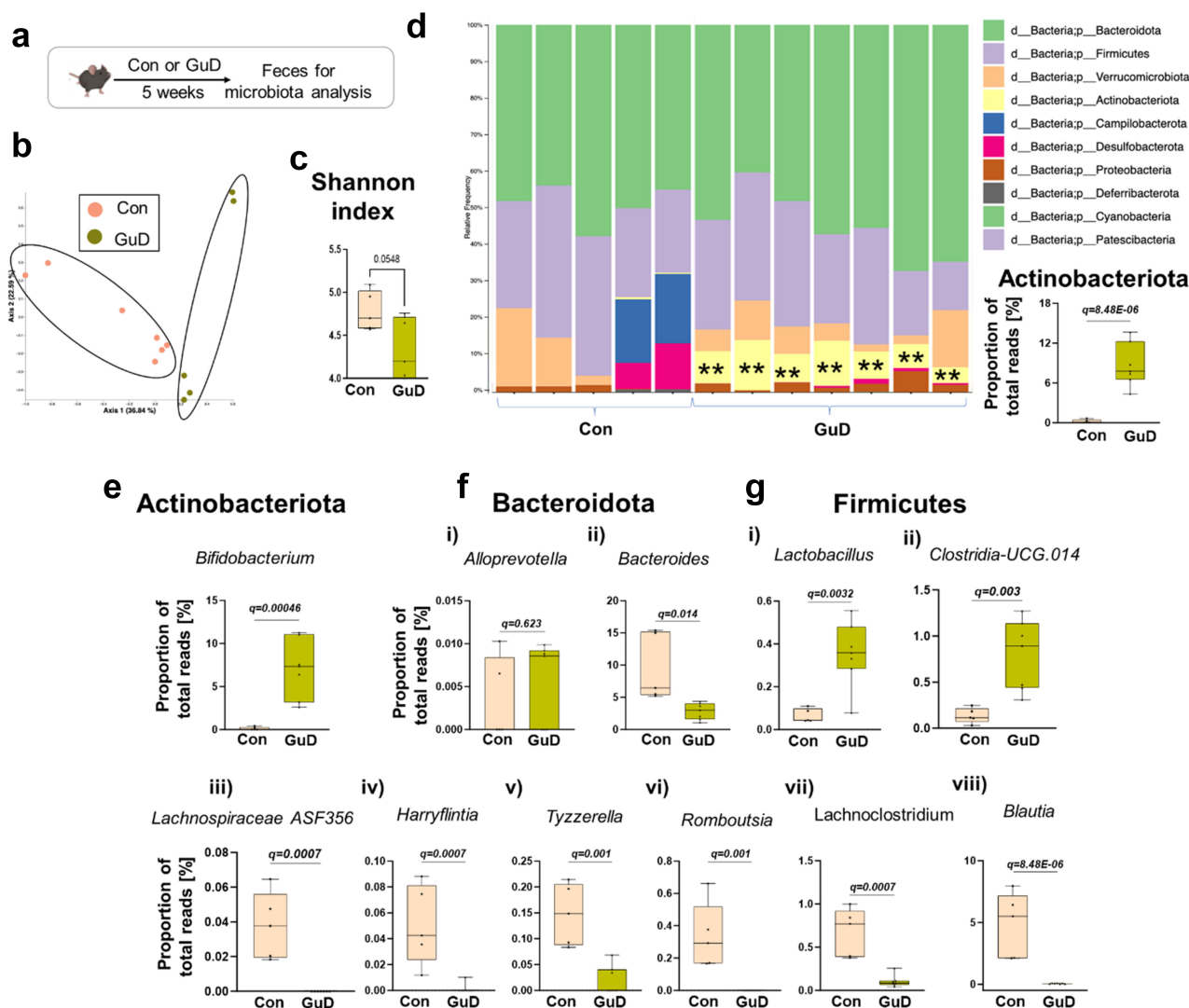


**Figure 3.** Guar gum fed mice displayed shift in gut microbiota enriching Actinobacteriota. (a) Experimental layout to study the shift in gut microbiota profile in guar gum (GuD) fed mice. Four-week-old WT mice ( $n = 5-7$  per group) maintained either on Con or GuD diet for 5 weeks. Feces were aseptically collected and used for 16S rRNA sequencing. (b-g) Microbial signature of control and GuD-fed mice. (b) Comparison of microbiota profiles by Principal coordinates analysis (PCoA) plot (c) Alpha diversity calculated by the Shannon index. (d) Relative abundance and distribution of microbial composition at the phylum level. The box plot represents the enrichment of Actinobacteriota following GuD intervention. (e-g) Mean relative abundance of conspicuously altered bacterial taxa at the genus level. The boxplot in each diagram represents the relative abundance plotted as a percentage of the total reads. Values are presented as mean  $\pm$  SEM. (d-g) Statistical analysis was performed using MaAsLin2 (Multivariate association with linear models) approach. The  $q$ -value (Benjamini-Hochberg false discovery rate corrected)  $< 0.05$  was considered as significant.

microbial metabolites influence intestinal immune homeostasis and gut barrier function. Therefore, we next quantified microbial metabolites in cecal contents through  $^1\text{H}$  NMR-based metabolomics to assess GuD-induced changes in microbial metabolites. Cecal level of SCFAs namely acetate, butyrate, and propionate remain unaltered (Figure 4(a)) in GuD-fed group when compared to control. The levels of branched chain amino acids (BCAAs) valine and isoleucine were significantly increased

in GuD-fed mice (Figure 4(b)). Notably, lactate, whose abnormal elevation in the intestinal lumen is associated with colitis severity<sup>37,38</sup> was augmented in the GuD-fed mice (Figure 4(c)). More importantly, we observed that luminal succinate, which fuels inflammatory signal through its receptor succinate receptor 1 (Succr1),<sup>13-15,39</sup> was substantially elevated ( $\sim 4$  folds) in cecal contents obtained from GuD-fed mice (Figure 4(d)). Such increase in luminal lactate and succinate in

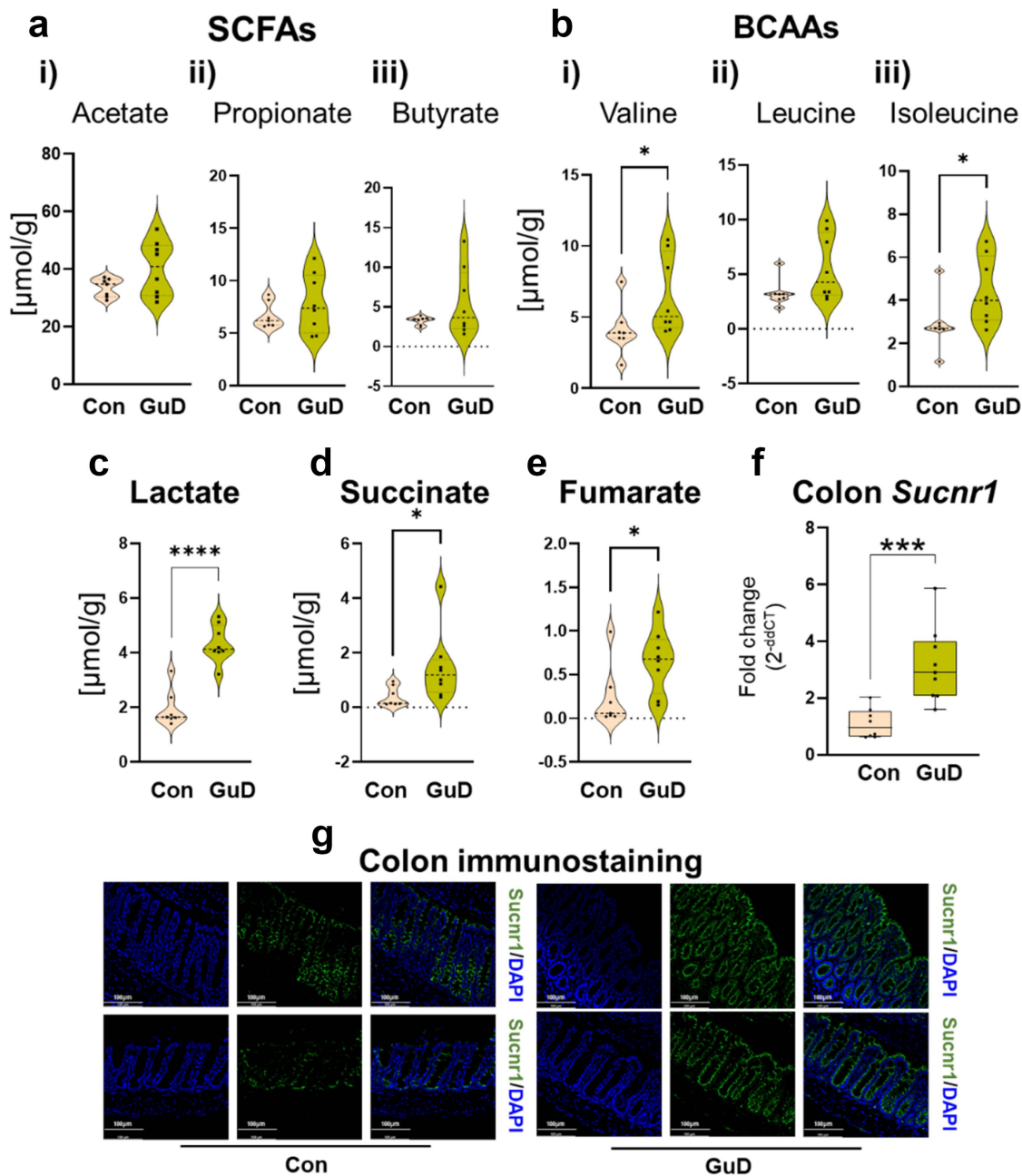


**Figure 4.** Guar gum-induced alterations in gut microbiota metabolism was associated with luminal accumulation of intermediate metabolites, including lactate and succinate. Four-week-old WT mice ( $n = 7-8$  per group) were maintained on either a Con or GuD diet for 5 weeks. Ceca (with cecal contents) were collected in a tube and snap-frozen immediately. About 50 mg of cecal content was used for metabolite analysis by using quantitative  $^1\text{H}$  NMR. The violin plots represent metabolites measured in  $\mu\text{mol/g}$  of cecal content. (a) Short chain fatty acids (SCFAs, acetate, propionate, and butyrate) (b) Branched-chain amino acids (BCAAs; valine, leucine, and isoleucine). (c) Lactate (d) Succinate (e) Fumarate. (f–g) Colon samples obtained from Con or GuD fed mice were used to determine (f) mRNA level of *Sucnr1*, and (g) colonic expression pattern of *Sucnr1* via immunohistochemistry. Values are presented as mean  $\pm$  SEM. (a–c and e–f) Unpaired t-test, (d) Unpaired non-parametric Mann–Whitney test. \*  $p < .05$ , \*\*  $p < .01$ , and \*\*\*  $p < .001$ .

response to guar gum intervention was aligned with an inordinate increase of their producers *Bifidobacterium* (>40 folds)<sup>32</sup> (Figure 3(e)) and *Lactobacillus* (>5 folds)<sup>40,41</sup> (Figure 3(gi)) and decreased abundance of their metabolizers

(*Bacteroides* and *Lachnoclostridium*) (Figure 3(fii) and gvii). Notably, higher succinate level within the gut lumen is reported to be associated with gut dysbiosis and potentiate colonic inflammation and is also augmented in patients with IBD.<sup>15,42</sup>



Succinate is typically low in the intestinal lumen as it is rapidly converted to an intermediate in the production of propionate.<sup>43,44</sup> However, we did not observe reduced propionate in the GuD-fed group. Microbial fermentation under low oxygen environment yields succinate primarily as a result of partial reversal of Krebs cycle reactions (reversed succinate dehydrogenase activity), where fumarate is converted to succinate (oxaloacetate → malate → fumarate → succinate).<sup>43,44</sup> We found increased levels of fumarate, the immediate precursor of succinate (Figure 4(e)), suggesting that partial reversal of TCA contributes to luminal succinate accumulation. Extracellular succinate is sensed by Sucnr1 (aka Gpr91), our mRNA expression and immunohistochemical analysis showed heightened colonic expression of succinate receptor Sucnr1 in GuD group (Figure 4(f,g)). Altogether, guar gum-induced atypical changes in gut microbiota promoted the accumulation of luminal metabolites commonly present in the inflamed gut.

### **Guar gum fed mice display altered expression of mucosal barrier markers and disruptive switch in mucosal immunity**

The mucus layer and intestinal epithelial lining form a critical line of defense. An intact mucosal barrier limits microbial invasion, fine-tunes the intestinal immune response, and prevents intestinal inflammation.<sup>45–47</sup> Therefore, we next assessed the effect of guar gum consumption on colonic mucins, epithelial junction molecules, and inflammatory markers. Quantitative polymerase chain reaction (qPCR)-based analysis revealed a reduced colonic mRNA level of membrane-associated mucin 1 (*Muc1*; also known as episialin) in GuD-fed group than control (Figure 5(a)). However, the expressions of secreted mucin, mucin 2 (*Muc2*), and of membrane-bound *Muc3* and *Muc4* were not significantly altered when compared to control (Figure 5(b–d)). The tight junction markers occludin (*Ocln*), zona occludin-1 (*Zo-1*), and members of claudins (*claudin-8* and *claudin-12*) were decreased in GuD-fed mice compared to the control group (Figure 5(e,f,k,l)). Notably, colonic expression of epithelial adherens *E-cadherin 1* was also reduced in GuD-fed group (Figure 5(m)). Conversely, the mRNA level of *claudin-3*

(Figure 5(i)) was elevated in GuD-fed mice. The expression of tight junction proteins, including claudin-1, claudin-2, and claudin-7, remained unaltered in response to GuD feeding (Figure 5(g,h,j)). Such differential alterations in mucosal barrier function markers in GuD-fed mice likely predisposed them to colitis. However, future studies are required to understand how guar gum-mediated alterations in colonic expression of these barrier function genes mediate susceptibility to colitis.

We next examined whether guar gum altered the colonic transcript levels of inflammatory genes at the baseline level (without inflammation). Comparison of immune markers in colonic tissue derived from control and GuD-fed mice revealed heightened expression of inducible nitric oxide synthase (*iNos*) with an increasing trend in interleukin-6 (*Il-6*) (Figure 6(a,b)). Surprisingly, colonic *Il-18* transcript level was reduced in GuD-fed mice (Figure 6(c)). Such decrease in IL-18 in mice fed GuD was confirmed by measuring in colon protein (Figure 6(d)) and via immunohistochemistry (Figure 6(e)). Jointly, our observations reported in Figures 5 and 6 revealed that the predisposition of guar gum-fed mice toward colitis was accompanied with reduced expression of colonic mucin and tight junction genes and increased expression of inflammatory gene. Intriguingly, colonic level of IL-18 was found substantially reduced at both mRNA and protein level.

### **Supplementation of IL-18 partly rescue guar gum-fed mice from colitis susceptibility**

Intestinal epithelium is a major producer of IL-18.<sup>48</sup> Studies using knockout mouse models and exogenous recombinant IL-18 (rIL-18) administration have shown both protective<sup>21,49</sup> and detrimental<sup>24</sup> effects of IL-18 on colitis. As reported above, we observed a decreased colonic IL-18 at both transcript and protein levels in GuD-fed mice. Colonic expression of IL-18, especially on epithelial cells, was also diminished in these mice. Therefore, to understand the contribution of guar gum-induced suppression of colonic IL-18 in increasing susceptibility to colitis, the rIL-18 was administered to a subgroup of mice maintained on GuD diet for 4 weeks (28 days). Specifically, rIL-18

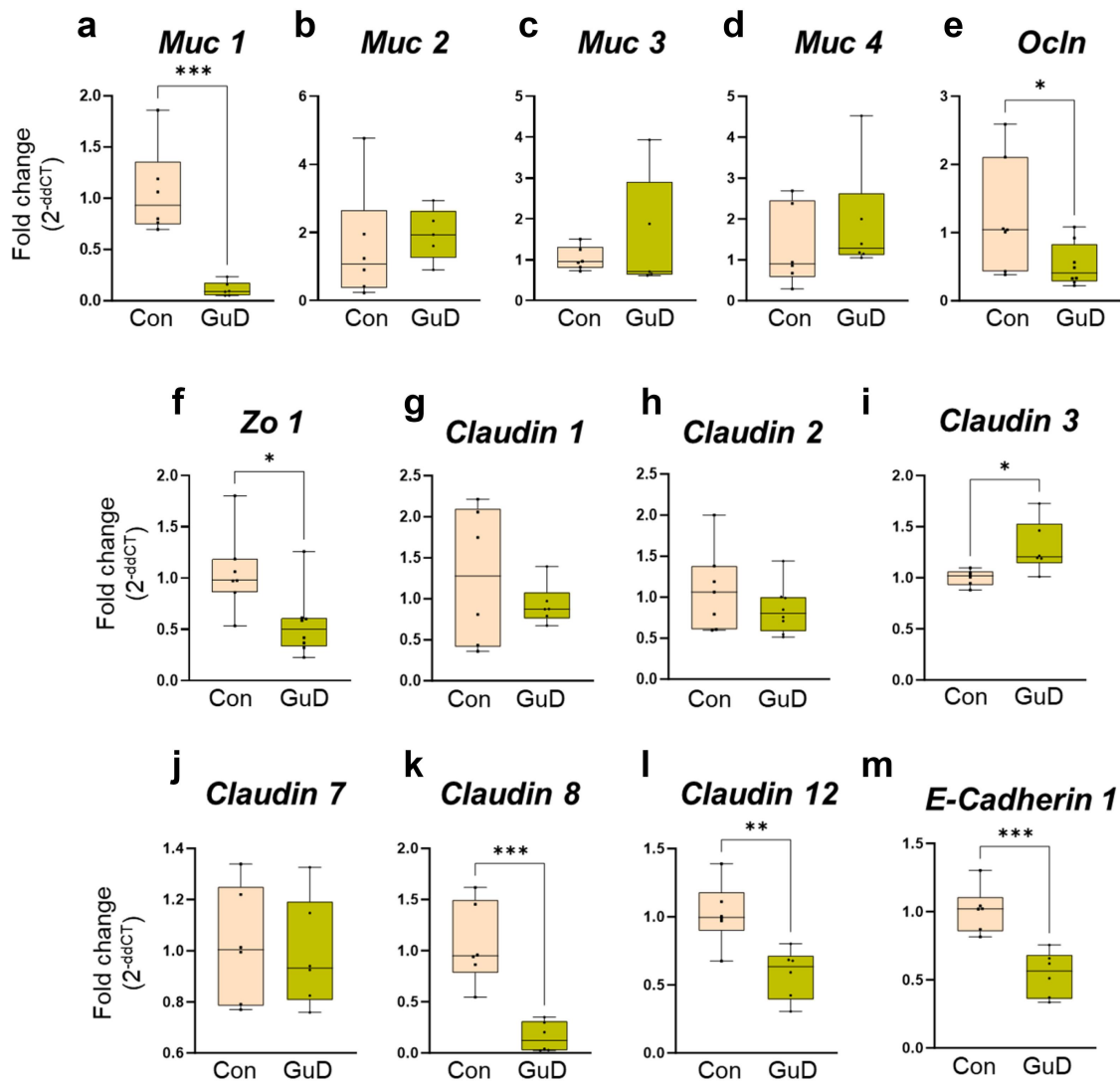


**Figure 5.** Guar gum suppressed the colonic mRNA expression of mucins and mucosal barrier proteins. Four weeks old WT mice ( $n = 5-6$  per group) maintained on Con or GuD diet for 5 weeks. Colonic mRNA expression of (a-d) mucins *Muc1*, *Muc2*, *Muc3*, and *Muc4*, (e-l) tight junction proteins *occludin* (*Ocln*), *zonula occludens-1* (*Zo 1*), and claudins, and (m) *E-cadherin 1*. Values are presented as mean  $\pm$  SEM. (a-m) Unpaired t-test. \*  $p < .05$ , \*\*  $p < .01$ , and \*\*\*  $p < .001$ .

was administered on days 29, 30, and 31, then mice were switched to DSS on day 34 or continued on water and monitored for colitis development for 1 week (Figure 7(a)). Relative to the vehicle-treated group, rIL-18 administration did in fact offer protection against DSS-induced colonic inflammation, as evidenced by recovery in body weight and decreased spleen weight (Figure 7(b-d)). As expected, the colon was shortened in the DSS-treated groups; however, the rIL-18 treatment did not exhibit a significant recovery in colon length (Figure 7(e)). Colonic *Lcn2* level was reduced in the GuD-fed mice supplemented with rIL-18 (Figure 7(f)). At the basal level, no significant

difference was observed in body weight, spleen weight, colon length, and *Lcn2* between vehicle and rIL-18-treated groups (Figure 7(b-f)). To further characterize the effect of rIL-18 administration on rescue from DSS-induced colonic inflammation, we examined colon Swiss roll sections *via* histochemical and immunohistochemical analysis. The colon sections from non-DSS treated GuD-fed mice with or without rIL-18 displayed intact crypt structure and mucin-containing goblet cells as evidenced by Alcian blue and *Muc2* immunostaining (Figure 7(g)). DSS-treated GuD-fed mice showed loss of crypt structure and extensive infiltration of immune cells in the submucosa. Notably, DSS-

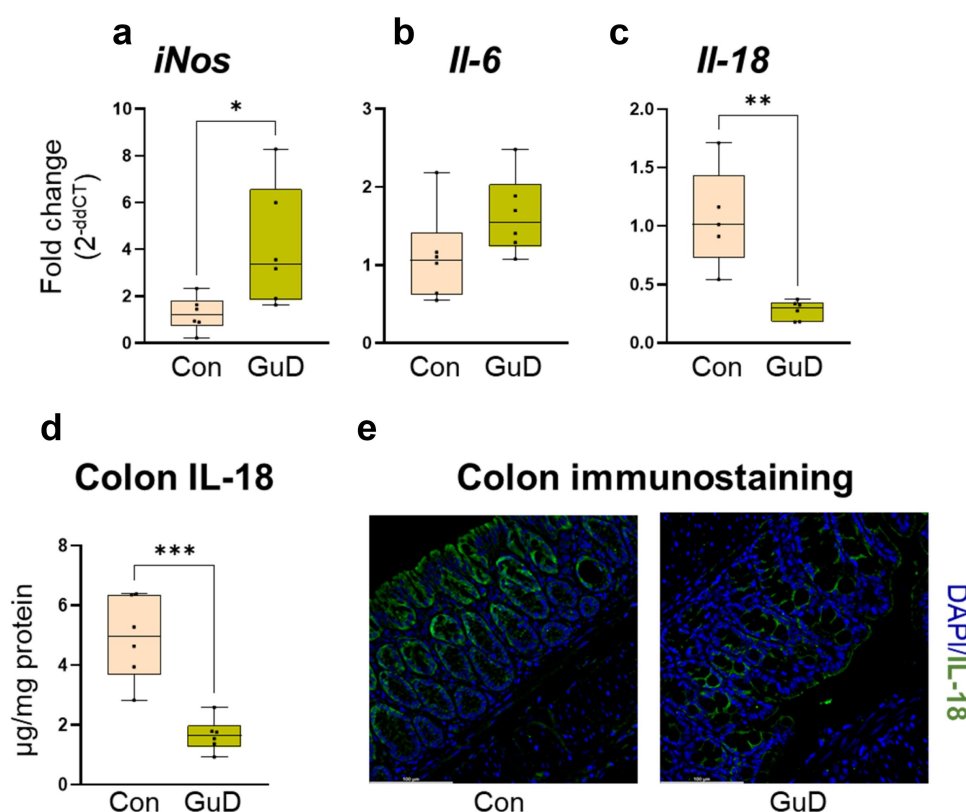


**Figure 6.** Guar gum-fed mice displayed reduced expression of colonic IL-18. Four weeks old WT mice ( $n = 4-5$  per group) maintained on Con or GuD diet for 5 weeks. After euthanasia, colonic tissue was collected for RNA and protein extraction and for immunohistochemical staining. (a-c) Colonic mRNA expression of *iNos*, *IL-6*, and *IL-18*. (d) Colonic IL-18 assessed by ELISA. (e) Representative images of colonic IL-18 immunostaining (green) (original magnification,  $\times 200$ ). Values are presented as mean  $\pm$  SEM. (a-d) Unpaired t-test. \*  $p < .05$ , \*\*  $p < .01$ , and \*\*\*  $p < .001$ .

treated GuD-fed mice that received rIL-18 displayed relatively low disruption of crypt structure and immune cell infiltration, higher numbers of mucin-containing goblet cells, and reduced colonic Lcn2 expression suggesting that pretreatment with rIL-18 partly prevented DSS-induced histological disruption (Figure 7(g,h)). Additionally, rIL-18 resulted in decreased serum levels of the inflammation markers Lcn2 and SAA (Figure 7(i,j)). Altogether, GuD-fed mice pretreated with rIL-18 displayed an improvement in overall disease severity score (Figure 7(k)). In order to determine whether GuD-mediated elevation of colonic *iNos* (Figure 6(a)) predisposes mice to colitis, we treated mice with the iNOS activity inhibitor 1400W and examined them for markers of DSS-induced colitis (Figure S3). Intriguingly, both the vehicle and 1400W-treated groups displayed comparable levels of colitis (Figure S3b-i), suggesting that iNOS induction in response to guar gum intervention is not contributing to colitis susceptibility in GuD-fed

mice. Collectively, the lack of improvement in colitis with iNOS activity inhibition and the amelioration of colonic inflammation upon pretreatment with rIL-18 supplementation strengthens the observation that reduced colonic IL-18 predisposes GuD-fed mice to colitis.

## Discussion

Health-beneficial properties of FDFs consumption have been reported for decades. However, the influence of different forms, structures, fermentation profiles, and physio-chemical properties of FDFs on intestinal inflammation have only recently begun to be understood.<sup>50-53</sup> FDFs serve as the primary nutrient source for the gut microbiota, and therefore offer the potential to modulate the composition and activity of the gut microbiota favorably. In the healthy gut, FDFs, including guar gum, have a beneficial effect on the composition of the microbiota.<sup>2-5</sup> Since

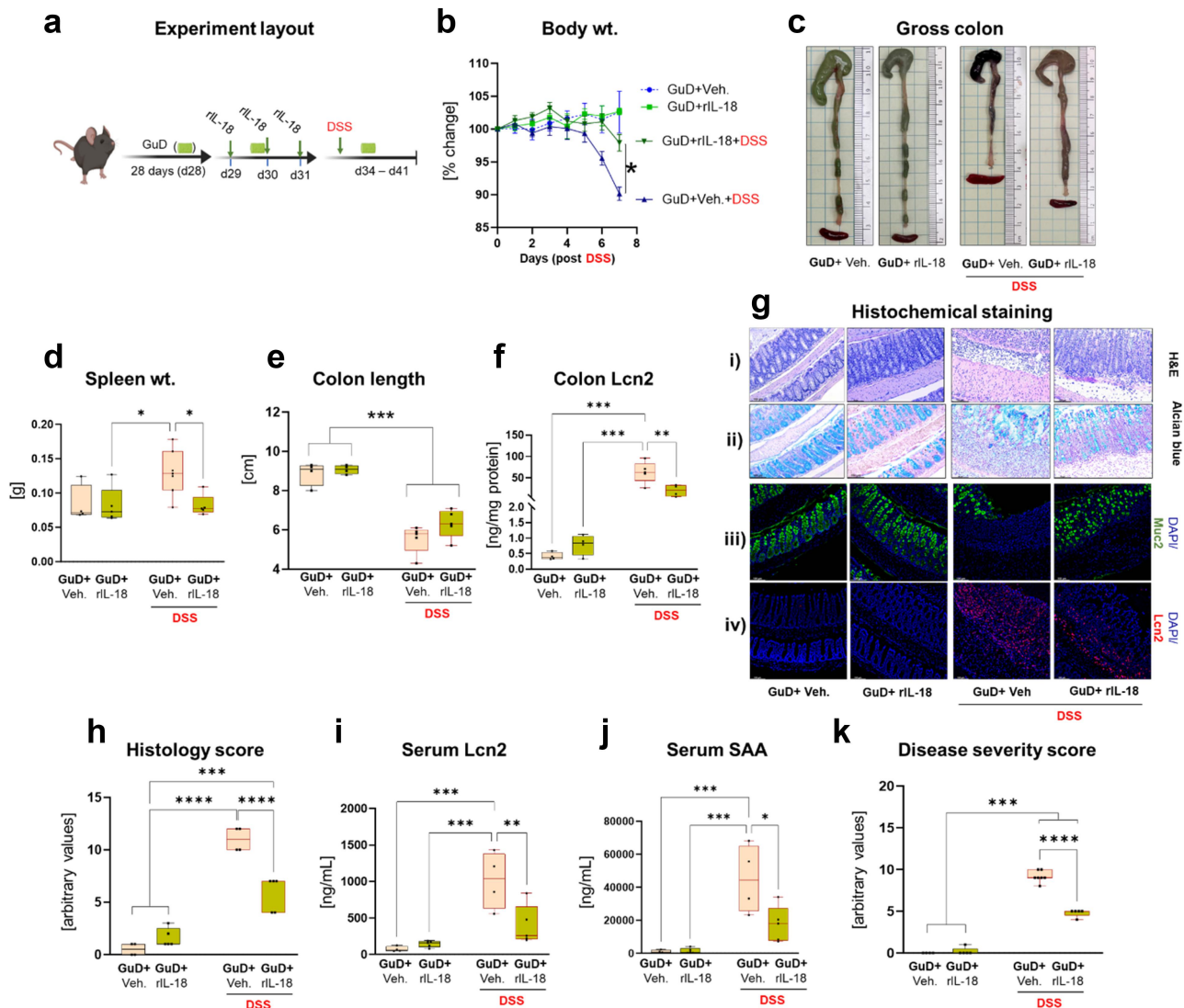


**Figure 7.** Exogenous IL-18 administration reduced GuD colitis severity in GuD-fed mice. (a) Experimental layout to assess the effect of exogenous recombinant IL-18 (rIL-18) on colitis severity. Four-week-old mice ( $n = 4-5$  per group) were maintained on a GuD for 4 weeks and were supplemented with vehicle (PBS) or rIL-18 at the dose of 1  $\mu\text{g}/\text{mouse}$  (in PBS) intraperitoneally for 3 consecutive days before switching them to DSS (1.4% w/v)-containing water or water only for 7 days. (b) Percent change in body wt. (c) Gross colon appearance. (d) Spleen wt. (e) Colon length. (f) Colonic Lcn2. (g i-iv) Representative images of colon sections stained with H&E (i) and Alcian blue (ii) (original magnification 100x). Colonic sections immunostained for Muc2 (iii, green) and Lcn2 (iv, red) (original magnification, 200x). (h) Histopathological scores derived from blinded evaluation of H&E-stained colonic sections. (i-j) Serum levels of (i) Lcn2 and (j) SAA. (k) Disease severity score. Values are presented as mean  $\pm$  SEM. (b) Unpaired t-test, (d-f and h-k) One-way ANOVA, multiple comparisons test. \* $p < .05$ , \*\* $p < .01$ , \*\*\* $p < .001$ , and \*\*\*\* $p < .0001$ .

a subgroup of patients with IBD report a poor tolerance and experience heightened inflammation upon consuming certain types of dietary fibers,<sup>52,54-56</sup> it is not well understood whether guar gum consumption benefits intestinal health during ongoing colonic inflammation, which is characterized by extensive dysbiosis. The present pre-clinical study advanced our understanding of FDF effects in the inflamed gut by demonstrating

that the food additive guar gum may exacerbate the clinical symptoms of IBD patients as it aggravated experimental colitis in a mouse model. We demonstrated that a shift in gut microbiota composition and activity as well as alterations in intestinal barrier function and immunity in response to guar gum intervention were associated with increased susceptibility to intestinal inflammation.



With the advent of the industrial revolution in 1800's, a shift in diet and lifestyle brought an increased consumption of processed foods which aligned with the appearance of IBD; by the end of the 20<sup>th</sup> century, the incidence and prevalence of IBD accelerated in both industrialized and newly industrialized countries.<sup>57</sup> An increased awareness among the general public about the health benefits of FDFs consumption in recent times has attracted food companies to fortify their products with extracted dietary fibers in order to validate their food functionality claims as beneficial for gut health. This continued emphasis on fiber use in the Western diet has led to the development of fiber-enriched products which are consumed by the general population on a daily basis, however, the implications of these refined fibers on people with or at risk of IBD is still not clear. Avoidance of fiber intake is generally recommended in practice when patients with IBD experience disease flare-ups, but these recommendations are not based on scientific evidence as our current understanding of the specific types of fibers to be avoided is limited.<sup>58</sup> In the present study, we examined the effect of guar gum, a commonly used food additive, on experimental colitis. To our surprise, guar gum exacerbated colonic inflammation induced by a colitogenic substance DSS. Although the exact causes of IBD are not yet known, disruption of microbiota composition and activity along with dysregulated immune response to gut microbiota are among the primary factors that increase susceptibility to IBD. Experimental mice pre-treated with the cocktail of antibiotics and antifungal agent displayed substantial attenuation of colitis in GuD-fed mice, implicating the potential involvement of gut microbiota in guar gum-mediated susceptibility to colitis. However, the lack of protection from DSS-induced colitis in the control group after similar intervention is surprising. While this suggests that gut microbiota and their metabolic activity may not be the primary drivers of colonic inflammation observed in the control group, other confounding factors, including antibiotic-mediated susceptibility to DSS-induced colitis, cannot be ruled out.<sup>59</sup> Intriguingly, antibiotic-treatment is shown to increase DSS-induced epithelial injury.<sup>59</sup> This study suggests that the amount of remaining microbiota (post-antibiotic intervention) and

regulatory T cells response modulate the severity of DSS-induced disease in antibiotic-treated mice. The extent to which control diet and guar gum differentially modulate microbiota composition and colonic immune response post antibiotic intervention requires further investigation. Collectively, the attenuation of DSS-induced colitis in antibiotic-treated GuD-fed mice reinforces our finding that altered microbiota composition and activity in the presence of guar gum potentiates colitis in mice. While the antibiotics intervention approach indicates the involvement of gut microbiota in guar gum-induced predisposition to colitis, it has certain limitations. These include incomplete elimination of gut microbiota and the inability to establish a causative role for gut microbiota in increased susceptibility to colitis in GuD-fed mice. Future studies involving fecal microbiota transplantation will be useful to determine the causal role of guar gum-induced gut microbiota dysbiosis in driving colitis susceptibility in GuD-fed mice. Given that the detrimental effects of guar gum on colonic inflammation are mediated by gut microbiota, we sought to investigate the guar gum-induced alterations in gut microbiota composition and their metabolic activity. Our results revealed important implications regarding how guar gum changed gut microbial composition unfavorably, predisposing the host to colitis susceptibility. At the phylum level, we observed inordinate expansion of phylum Actinobacteriota compared to the control group. Precisely, expansion of *Bifidobacterium* contributed to excessive increase of Actinobacteriota in guar gum-fed mice. The taxonomic shift with the enrichment of Actinobacteriota is also observed in patients with IBD.<sup>60</sup> *B. pseudolongum* belonging to genus *Bifidobacterium* are generally considered anti-inflammatory and has shown to ameliorate disease severity in experimental mouse models of ulcerative colitis.<sup>61</sup> Opposingly, increased abundance of *Bifidobacterium* and *Lactobacillus* along with loss of butyrate producing bacteria has been reported in patients with active IBD cautioning its use as probiotics during diseased state.<sup>62</sup> Further analysis of gut microbiota composition revealed that guar gum-induced genus-level alterations in phyla Bacteroidota and Firmicutes favoring the enrichment of intermediate metabolite such as lactate and succinate by promoting expansion of

succinate and lactate producer (*Bifidobacterium* and *Lactobacillus*),<sup>63–65</sup> and reducing their utilizer (*Bacteroides*).<sup>63,64,66</sup> The cross-feeding of intermediate metabolites is an integral part of a highly diverse healthy microbiota.<sup>67</sup> Specifically, lactate and succinate subsequently fermented into SCFAs<sup>43, 64–66</sup>, chief end products of DF fermentation. Therefore, accumulation of succinate and lactate in the intestinal lumen of guar gum fed mice indicating disrupted gut microbiota metabolism and cross-feeding relationships.<sup>17,63</sup> Moreover, microbial cross-feeding has a significant impact on the SCFA levels in the ceca. Therefore, the luminal accumulation of these intermediate metabolites explains why SCFA levels remained unaltered in the GuD-fed mice. Previous studies have shown elevated succinate in IBD and pointed to the pro-inflammatory role of succinate.<sup>13</sup> Succinate signals G-protein coupled receptors include *Sucnr1*, whose expression is increased in pro-inflammatory macrophages.<sup>68</sup> Deletion of *Sucnr1* has a protective effect against intestinal inflammation.<sup>15</sup> We observed an increase in colonic expression of succinate receptor *Sucnr1* in the GuD-fed mice, suggesting that elevated succinate possibly potentiating the intestinal inflammation through engaging *Sucnr1*. In the intestinal lumen, lactate is formed as an intermediate product of fiber fermentation. Intestinal bacteria further ferment lactate into SCFAs.<sup>43,63,64</sup> Accumulation of luminal lactate is viewed as gut microbiota dysbiosis, including disturbed cross-feeding interactions among the microbes. Patients with IBD display elevated systemic and fecal lactate<sup>38,69,70</sup> and, in the context of intestinal inflammation, lactate can play a role in both the initiation and perpetuation of the inflammatory response.<sup>70,71</sup>

In a continuing effort to identify how guar gum perturbed gut microbiota increased susceptibility to colitis, we examined alterations in intestinal barrier function and immune markers at the basal level. Such analysis revealed reduced colonic expression of tight junction markers and elevated mRNA level of *Nos2*, encoding inducible nitric oxide synthase (iNOS). Augmented colonic iNOS activity is shown to exacerbate colitis.<sup>72</sup> Intriguingly, intervention with 1400W, a selective inhibitor of iNOS,<sup>73</sup> did not impact the progression of DSS-induced colitis in GuD-fed mice. This

suggests that elevated colonic iNOS in response to guar gum feeding might not be contributing to increased colitis susceptibility. Notably, the colonic IL-18 was substantially reduced in mice received guar gum. Whether intestinal IL-18 promotes or attenuates intestinal inflammation remains controversial. IL-18 is continuously produced by intestinal epithelial cells basally and participate in regulating intestinal epithelium regeneration<sup>20</sup> and immune activity.<sup>18</sup> An elegant study by Nowarski et. al,<sup>24</sup> using IL-18 signaling related multiple KO mouse models, including epithelial cell-specific KO showed that IL-18 promote colitis. Recently, another elegant study by Chiang HY<sup>20</sup> showed that IL-18 mediates IL-22 dependent protective effect by increasing host defense. In fact, IL-18<sup>-/-</sup> mice were found to be more susceptible to AIEC infection with impaired bacterial clearance. Such opposing effects of IL-18 on intestinal inflammation have been observed in multiple studies, either using knockouts or administering recombinant IL-18 exogenously. In our study, colonic IL-18 was reduced in mice fed guar gum, and GuD-fed mice that received rIL-18 were rescued from DSS-induced colitis. This indicates that guar gum-mediated suppression of colonic IL-18 predisposed GuD-fed mice to colitis. In agreement, a study by Iljazovic A et al.,<sup>21</sup> found a protective effect of rIL-18 administration on the severity of colonic inflammation in mice. Herein, authors observed that colonization of mice with *Prevotella intestinalis* suppressed colonic IL-18 levels before induction of intestinal inflammation.<sup>21</sup> In our study, *Alloprevotella*, belonging to the same family Prevotellaceae, was comparable between control and guar gum-fed mice, suggesting that suppression of colonic IL-18 occurred through another mechanism and warrants further investigation to elucidate the precise mechanism of colonic IL-18 suppression. The role of IL-18 in colonic inflammation may be time-dependent with IL-18 having a protective role in early stages of disease and a detrimental effect in later stages. A study found that pretreatment with IL-18 before DSS administration was associated with reduced inflammation while later treatment with IL-18 in mice with DSS-induced colitis led to increased inflammation.<sup>23</sup> Additionally, IL-18 is found to upregulate IL-22, which is involved in epithelial repair.<sup>23</sup> Altogether,

some studies have shown a protective role of IL-18 while others observed that IL-18 may exacerbate the severity of colonic inflammation<sup>21</sup>. While our results in combination with existing studies showed protective effect of exogenous IL-18, the role of endogenous IL-18 in DSS-induced colitis is poorly understood. Pretreating mice with IL-18 can attenuate DSS-induced colitis,<sup>23</sup> therefore, observed amelioration of colitis in IL-18 treated GuD-fed mice before DSS intervention might be a general effect of IL-18 on DSS-induced colitis. The role of reduced IL-18 at later stages of colitis in response to guar gum feeding requires further investigation.

Guar gum-induced shifts in microbiota composition led to the accumulation of lactate and succinate in the intestinal lumen. Such abnormal accumulation of these intermediate metabolites, along with altered gut barrier function and disrupted immune homeostasis (reduced colonic IL-18), collectively increased susceptibility to colitis in guar gum-fed mice. While our study provides caution against refined guar gum consumption in a subset of the population, such as patients with active IBD or people with a higher risk of developing IBD. Further research is required, especially randomized clinical trials or population-based studies that can better demonstrate the effects of guar gum consumption on IBD-associated complications in the human population. More investigation into the role of guar gum-induced alterations in microbial activity, particularly in the inflamed intestine, will result in a better understanding of the dietary fiber – gut microbiota interaction and its impact on IBD development. A higher predisposition to develop colitis upon guar gum consumption is particularly important as guar gum is chiefly added to ultra-processed foods, which are also linked with increased IBD susceptibility.<sup>74,75</sup> Therefore, consumption of processed food containing guar gum may pose a relatively higher risk of developing IBD in the long run.

## Materials and methods

### Mice and diets

C57BL/6 background, Wild type (WT) mice were bred and maintained under specific pathogen-free

conditions at The Pennsylvania State University, University Park, Pennsylvania. Mice were bred and housed in cages (4-5 mice/cage) with corn cob bedding and nestlets. The mice had unrestricted access to food and water. The conditions of the experiments were approved by the Institutional Animal Care and Use Committee at The Pennsylvania State University. The minimum number of mice per genotype to achieve statistically significant data through sample size calculation was determined to be 4–7 ( $\alpha = 0.05$ ,  $\beta = 0.80$ ). The experimental diets were prepared by the Research Diets, Inc. (New Brunswick, NJ) where guar gum fiber was supplied by TIC Gums Inc, MD, USA (88% purity). Composition of all diets including the source of dietary fibers cellulose and guar gum are provided in [Table 1](#).

### DSS-induced colitis

WT mice (male or female; 4–5 weeks old; diet only group ( $n = 6-7$ ) and diet + DSS group ( $n = 6-8$ )) were maintained on control (Con) (10% cellulose w/w) or guar gum (GuD) containing diet (7.5% GuD + 2.5% Con w/w) for four weeks. Then, colonic inflammation was induced by the administration of 1.4% DSS (w/v) through drinking water for 7 days. All mice were maintained on respective fiber containing diets during DSS administration period. Body weight, severity of disease symptoms such as soft feces, traces of blood in feces and mild diarrhea were monitored as a readout for colitis. On day 7<sup>th</sup> of DSS treatment, mice were euthanized for sample collection. To investigate the effect of guar gum on acute colitis, physiological and metabolic changes in the gut, expression of pro-inflammatory cytokines such as lipocalin 2 and serum amyloid A (SAA), gross colon appearance, colon length, spleen weight, body weight and histochemical staining were examined.

### Broad-spectrum antibiotic mixture administration

WT, male mice ( $n = 4-6$  per group) were maintained on chow diet until 6 weeks of age. Then, mice in the treatment group were provided with broad spectrum antibiotics through drinking water for 4 weeks with a chow diet for 1 week and GuD containing diet for 3 weeks. Mice in the control

group were treated similarly without antibiotics. The antibiotics mixture was comprised of broad-spectrum antibiotics [Ampicillin (1 g/L), Neomycin (1 g/L), Metronidazole (1 g/L), Vancomycin (0.5 g/L)] and an antifungal agent [Amphotericin B (10 mg/L)]. After 3 weeks, antibiotics administration was discontinued and both groups were intervened with 1.4% DSS through drinking water for 7 days to induce colonic inflammation. On the 7th day, mice were euthanized for sample collection. Body weight, severity of disease symptoms such as soft feces, traces of blood in feces and mild diarrhea were monitored as a readout for clinical outcomes.

### **Intervention with recombinant IL-18 (rIL-18)**

Four-week-old WT mice were fed a GuD for four weeks and then divided into four groups ( $n = 4-6$  per group). The rIL-18 intervention procedure was adopted from the studies by Seregin SS et al.<sup>76</sup> and Levy M et al.<sup>22</sup> From days 29 to 31, two groups received either recombinant mouse interleukin-18 (rIL-18, 1 µg/mouse; BioLegend), and another two groups received vehicle (veh.) intraperitoneally (i. p.). After 2 days of last injection, experimental groups were either switched to DSS (1.4% w/v) containing water (GuD+ veh. + DSS and GuD+ rIL-18+ DSS) or continued on regular water (GuD+ veh.+ water and GuD+ rIL-18+ water). After 7 days of DSS administration, mice were euthanized to collect samples for analyzing colitis markers. Mice were maintained on the GuD throughout the study.

### **Treatment with iNOS inhibitor 1400W**

As described in the rIL-18 intervention procedure above, mice were regrouped into two groups after 4

weeks of GuD feeding ( $n = 4-6$  per group). Next, both groups received seven i.p. injections (one per day) of either veh. or selective iNOS inhibitor *N*-[3-(aminomethyl) benzyl] acetamidine (1400W, Calbiochem) at a dose of 5 mg/Kg body weight. After the 1st injection, one group of mice was administered with DSS (1.4% w/v), while the other group remained on drinking water. Seven day-post DSS administration, both groups were euthanized for sample collection and subsequent analysis. All groups of mice received GuD throughout the experimental period.

### **Mouse euthanasia and sample collection**

The experimental mice were euthanized by exposing to carbon dioxide (CO<sub>2</sub>). Blood was then collected from the portal vein and transferred into serum separator tubes (Becton Dickinson). Centrifugation of blood in serum separator tubes yielded hemolysis-free serum. Colonic tissues were flushed with ice cold PBS and immediately transferred to container containing liquid nitrogen or dry ice for protein extraction. Colon tissues for RNA analysis was stored at  $-20^{\circ}\text{C}$  in RNA later solution (Sigma Aldrich). For colon histology, Swiss-rolls were formed from proximal to distal end followed by transferring to neutral buffered formalin (NBF) for 24 hours. Subsequently, colons were placed in 70% ethanol and then submitted to Penn State University animal diagnostic laboratory facility for embedding in paraffin blocks, generating 5 µm cross-sections and for hematoxylin and eosin (H&E) staining.

### **Disease severity assessment**

To assess colonic inflammation severity, a composite disease severity scoring scheme was developed based on previously described

**Table 2.** Composite scoring system for assessing disease severity.

Weight loss (%) compared to the initial body weight		Histopathology score (on a scale of 0–12)		Presence of blood in feces and stool consistency (± diarrhea)	
Range (%)	Score	Range	Score	Observation	Score
0 to 4.9	0	<2	0	Blood traces in feces and diarrhea: Not observed	0
5 to 9.9	1	2.1–3.9	1	Blood traces or diarrhea: Yes	2
10 to 14.9	2	4.0–6.9	2		
15–18.9	3	7–9.9	3	Blood traces in feces and diarrhea: Yes	4
>19	4	>10	4		



methods<sup>77,78</sup> with slight modifications. As outlined in Table 2, a score of 0–4 was assigned for each marker: 1) weight loss compared to initial weight, 2) stool consistency (presence/absence of diarrhea), 3) presence of blood in feces, and 4) histology score. The final scores were calculated by summing the scores for each marker.

### RNA isolation cDNA preparation and quantitative polymerase chain reaction (PCR)

Quantitative PCR (qPCR) was utilized to assess the expression of colonic genes encoding immune function and tight junction markers. Briefly, colon tissues stored in RNA later (Sigma) solution was used to extract total RNA and converted into complementary DNA (cDNA) by using an RNA extraction kit (GE Healthcare) and qScript™ XLT cDNA supermix kit (QuantaBio), respectively, as per manufacturer's protocol. The concentration and purity of extracted RNA were determined by NanoDrop spectrophotometer (Thermo Scientific). One microgram (1 µg) of RNA was reverse transcribed to prepare cDNA. The expression of genes that encode immune function and tight junction markers was measured by using QuantStudio 3 Real-Time PCR System (Applied Biosystems). Primer sequences for genes assessed in this study are listed in Table 3. The difference in transcript levels was quantified through normalization with

housekeeping gene *36B4*, and the data are reported as  $2^{-\Delta\Delta CT}$ .

### Enzyme-linked immunosorbent assay (ELISA)

Colon tissue was homogenized in extraction buffer (containing 50 mM Tris, pH 7.4, 250 mM NaCl, 5 mM EDTA, 50 mM NaF, 1 mM Na<sub>3</sub>VO<sub>4</sub>, and 1% detergent; Invitrogen™) supplemented with protease inhibitor cocktail (Roche). The colon homogenates were then centrifuged at 13,000×g for 12 minutes at 4°C, and the supernatant was stored at –80°C until analysis. The level of colonic IL-18 and Lcn2 and serum SAA and Lcn2 were measured by ELISA as per manufacturer's procedure (R&D Systems). The level of colonic IL-18 and Lcn2 were normalized to tissue protein content and presented as per mg tissue protein.

### Histochemical and immunohistochemical staining

For histochemical staining, paraffin-embedded colonic sections were deparaffinized using a Leica autostainer XL (Leica Biosystems). H&E-stained sections were used to evaluate changes in crypt structure, ulceration, thickening of mucosa, hyperplasia, and immune cell infiltration. As per the manufacturer's protocol, Alcian blue staining was performed in deparaffinized sections to identify goblet cells containing acidic mucus using the Alcian Blue Stain Kit (Vector Laboratories Inc). Next, different sets of colon sections were used for immunohistochemical staining to assess the

**Table 3.** Primer sequences.

Target genes	Forward (3'—5')	Reverse (5'—3')	Reference
<i>36B4</i>	GAAAGAAGCCGAGGACCAC	TCTGTCACCGCCTTACCAAT	79
<i>Sucnr1</i>	ACAGAAGCCGACAGCAGAAT	GCACAGGAAAGCAAAGTCAG	80
<i>Muc1</i>	CCCTACCTACCACACTCAGGACG	GTGGTCACCACAGCTGGGTTGGTA	81
<i>Muc2</i>	AAGTACAGATCAAGACCGTGAGG	CCACTAACTGCTTGTTCACTG	81
<i>Muc3</i>	CGTGGTCAACTGCGAGAATGG	CGGCTCTATCTCTACGCTCTCC	76
<i>Muc4</i>	GAGGGCTACTGTCACAATGGAGGC	AGGGTTCCGAAGAGGATCCCGTAG	81
<i>Claudin-1</i>	CAACCCGAGCCTTGATGGTA	ACTAATGTCGCCAGACCTGA	82
<i>Claudin-2</i>	GTCATCGCCCATCAGAAGAT	ACTGTTGGACAGGGAACCA	83
<i>Claudin-3</i>	TCATCGGCAGCAGCATCATCAC	ACGATGGTGATCTTGGCCTTGG	84
<i>Claudin-7</i>	AGGGTCTGCTCTGGTCCTT	GTACGCAGCTTTGCTTTCA	85
<i>Claudin-8</i>	GCCGGAATCATCTTCTTCAT	CATCCACAGTGGGTTGTAG	85
<i>Claudin-12</i>	GTCCTCTCTTTCTGGAAC	ATGTCGATTTCATGGCAGA	85
<i>Occludin</i>	ATGTCCGGCCGATGCTCTC	TTTGGCTGCTCTGGGCTGTAT	83
<i>E Cadherin-1</i>	ACTTGGGGACAGCAACATCA	GGGTTTAAATCGGCCAGCA	86
<i>Zonula occludens-1</i>	ACCCGAAACTGATGCTGTGGATAG	AAATGGCCGGGAGAACTTGTGA	83
<i>iNos</i>	CTTTGCCACGGACGAGAC	TCATTGTACTCTGAGGGCTGAC	87
<i>IL-6</i>	CCACTTCAAGTCGGAGGCTTA	GCAAGTGCATCATCGTTGTCATAC	88
<i>IL-18</i>	CATGTACAAAGACAGTGAAGTAAGAGG	TTTCAGGTGGATCCATTTC	89

expression of mucin 2 (MUC2, Abcam), Lcn2 (R&D Systems) and IL-18 (Invitrogen). Specifically, sections were first deparaffinized then antigen retrieval was performed by transferring slides to pre-warmed sodium citrate buffer (pH 6.0) and allowing incubation at 98°C for 20 minutes in a water bath. After cooling down and washing with PBS, the nonspecific sites were blocked by incubating the sections with 10% donkey serum containing 0.3% Triton X-100 (VWR Life Sciences) for 90 minutes at room temperature. Primary antibodies (Lcn2, IL-18 or MUC2) were diluted in PBS containing 1% bovine serum albumin (BSA) and 0.3% Triton X-100 and applied on sections and incubated at 4°C overnight. Subsequently, sections were washed with PBS and incubated with secondary antibody Alexa Fluor 488 (anti-rabbit IgG) for 90 minutes at 37°C. Tissues were mounted with an antifade reagent containing 4',6'-diamidino-2-phenylindole (DAPI) for DNA staining. All the images were captured using a Leica DMi8 microscope (Leica Microsystems).

### **Histopathologic assessment**

Histological scoring was blindly determined on each colon as previously described.<sup>26,90</sup> Briefly, each colon was assigned four scores based on the degree of epithelial damage and inflammatory infiltration in the mucosa, submucosa, and muscularis/serosa.<sup>90</sup> Each of the four scores was multiplied by a coefficient 1 if the change was focal, 2 if it was patchy and 3 if it was diffuse<sup>26</sup> and the 4 individual scores per colon were added, resulting in a total scoring range of 0–36 per mouse.

### **Assessment of metabolites by <sup>1</sup>H NMR-based metabolomics**

NMR-based metabolomics was used to quantify the metabolites in cecal contents (~50 mg) obtained from control and GuD-fed mice. As described in our previous studies,<sup>53,91–94</sup> the <sup>1</sup>H spectra of cecal content extracts were recorded at 298 K using a Bruker Avance NEO 600 MHz spectrometer (Bruker Biospin) equipped with a 5 mm TCI cryoprobe and a SampleJet sample changer. The noesyppr1d pulse sequence was used for

recording <sup>1</sup>H 1D experiments with pre-saturation water suppression during relaxation and mixing time. The used parameters were: spectral width 20 ppm, time domain data points 64 K, acquisition time 2.75 s, relaxation delay 5 s, mixing time 100 ms, number of scans 64 with dummy scans 4. All <sup>1</sup>H NMR spectra were processed automatically with Chenomx NMR Suite (Chenomx Inc. version 10), then were checked and adjusted manually for phase, baseline, and chemical shift reference (TMSP, at 0.00 ppm) for each spectrum for meeting quality requirements. The metabolites were identified and fit using the in-built library and the metabolite concentration was calculated according to internal standard (TMSP, 0.29 mM).

### **Microbiota analysis through 16S rRNA gene sequencing**

16S rRNA gene amplification and sequencing were performed using the Illumina MiSeq technology following the protocol of the Earth Microbiome Project ([www.earthmicrobiome.org/emp-standardprotocols](http://www.earthmicrobiome.org/emp-standardprotocols)),<sup>95</sup> with some modifications. Briefly, the 16S rRNA genes, region V4, were PCR amplified from each sample using a composite forward and reverse primer containing a unique 12-base barcode, designed with the Golay error-correcting scheme used to tag PCR products from respective samples.<sup>95</sup> The forward primer 515F was used 5'-AATGATACGGCGACCACCGAGATCTACACGCTXXXXXXXXXXXXTATGGTAATTGTGTGYCAGCMGCCGCGGTAA-3': the italicized sequence is the 5' Illumina adapter, the 12X sequence is the Golay barcode and the bold sequence is the primer pad, the italicized a bold sequence is the primer linker and the underlined sequence is the conserved bacterial primer 515F. The 806 R primer used was 5'-CAAGCAGAAGACGGCATACGAGATAGTCAGCCAGCCGGACTACNVGGGTWTCTAAT-3': the italicized sequence is the 3' reverse complement sequence of Illumina adapter, the bold sequence is the primer pad, the italicized and bold sequence is the primer linker and the underlined sequence is the conserved bacterial primer 806 R. PCR reactions consisted of 5PRIME HotMasterMix (Quantabio, Beverly, MA, USA) 0.2 μM of each primer, 10–100 ng template, and reaction

conditions were set as follow: 3 min at 95°C, followed by 30 cycles of 45 s at 95°C, 60 s at 50°C and 90 s at 72°C on a Biorad thermocycler. PCR products were then visualized by gel electrophoresis and quantified using Quanti-iT PicoGreen dsDNA assay). A master DNA pool was generated from the purified products in equimolar ratios, and subsequently purified with Ampure magnetic purification beads (Agencourt, Brea, CA, USA). The obtained purified pool was quantified with the Quanti-iT PicoGreen dsDNA assay, followed by sequencing using an Illumina MiSeq sequencer (pair-end reads, 2 × 250bp) at the GENOM'IC core facility at Cochin Institut, Paris, France.

### 16S rRNA gene sequence analysis

QIIME2-version 2022 was used to analyze 16S rRNA sequences.<sup>96</sup> These sequences were demultiplexed and quality filtered using Dada2 method<sup>97</sup> with QIIME2 default parameters to detect and correct Illumina amplicon sequence data, generating a table of Qiime 2 artifact. Then, a tree was generated using the align-to-tree-mafft-fasttree command for phylogenetic diversity analysis and we computed alpha and beta diversity parameters using the core-metrics-phylogenetic command. Principal Coordinate Analysis (PCoA) plots were used to assess variations between experimental groups (beta diversity). Alpha diversity was computed with the Evenness index. For the taxonomic analyzes, features were assigned to operational taxonomic units (OTUs) with a 99% threshold of pairwise identity to the SILVA reference database. We employed the Microbiome Multivariable Associations with Linear Models (MaAsLin2) approach to identify differentially abundant microbial communities.<sup>98</sup> Unprocessed sequencing data are deposited in the European Nucleotide Archive under accession number PRJEB64411.

### Statistical analysis

The normal distribution of the data was tested via the D-Agostino-Pearson omnibus normality test. Data are represented as the Mean ± Standard Error of the Mean (SEM). An unpaired, two-tailed t-test was used to test the statistical significance between two groups. If more than two

groups were compared, a one-way ANOVA test followed by Tukey's multiple comparison tests were used. Any *p* value less than 0.05 was deemed statistically significant. GraphPad Prism 7.0 program (GraphPad, Inc.) was used to perform all statistical analyzes.

### Acknowledgments

The authors thank the Genom'IC platform (Institut Cochin, Paris, France) for its help in Illumina sequencing.

### Disclosure statement

No potential conflict of interest was reported by the author(s).

### Funding

This work was supported by Career Development Award [ID# 597229] from Crohn's and Colitis Foundation and NIH award [R01DK133334-01A1]. D.P. was supported by NIH grant [T32DK120509]. BC's laboratory is supported by a Starting Grant from the European Research Council (ERC) under the European Union's Horizon 2020 research and innovation program (grant agreement No. [ERC-2018-StG- 804135], a Chaire d'Excellence from IdEx Université de Paris - ANR-18-IDEX-0001, an Innovator Award from the Kenneth Rainin Foundation, an award from the Fondation de l'Avenir [AP-RM-21-032], ANR grants EMULBIONT [ANR-21-CE15-0042-01] and DREAM [ANR-20-PAMR-0002] and the national program "Microbiote" from INSERM.

### ORCID

Vishal Singh  <http://orcid.org/0000-0003-3577-1713>

### Data availability statement

The microbiota sequencing data that support the findings of this study will be openly available in the European Nucleotide Archive under accession number PRJEB64411.

### References

1. Mudgil D, Barak S, Khatkar BS. Guar gum: processing, properties and food applications—A review. *J Food Sci Technol*. 2014;51(3):409–418. doi:10.1007/s13197-011-0522-x.
2. Yasukawa Z, Inoue R, Ozeki M, Okubo T, Takagi T, Honda A, Naito Y. Effect of repeated consumption of partially hydrolyzed guar gum on fecal characteristics and gut microbiota: a randomized, double-blind,

- placebo-controlled, and parallel-group clinical trial. *Nutrients*. 2019;11(9):11. doi:10.3390/nu11092170.
3. Chen Y, Wan M, Zhong Y, Gao T, Zhang Y, Yan F, Huang D, Wu Y, Weng Z. Partially hydrolyzed guar gum modulates gut microbiota, regulates the levels of neurotransmitters, and prevents CUMS-induced depressive-like behavior in mice. *Mol Nutr Food Res*. 2021;65(16):e2100146. doi:10.1002/mnfr.202100146.
  4. Fu X, Li R, Zhang T, Li M, Mou H. Study on the ability of partially hydrolyzed guar gum to modulate the gut microbiota and relieve constipation. *J Food Biochem*. 2019;43(2):e12715. doi:10.1111/jfbc.12715.
  5. Liu X, Wu C, Han D, Liu J, Liu H, Jiang Z. Partially hydrolyzed guar gum attenuates d-galactose-induced oxidative stress and restores gut microbiota in rats. *Int J Mol Sci*. 2019;20(19):20. doi:10.3390/ijms20194861.
  6. Ahlawat S, Kumar P, Mohan H, Goyal S, Sharma KK. Inflammatory bowel disease: tri-directional relationship between microbiota, immune system and intestinal epithelium. *Crit Rev Microbiol*. 2021;47(2):254–273. doi:10.1080/1040841X.2021.1876631.
  7. Franzosa EA, Sirota-Madi A, Avila-Pacheco J, Fornelos N, Haiser HJ, Reinker S, Vatanen T, Hall AB, Mallick H, McIver LJ. et al. Gut microbiome structure and metabolic activity in inflammatory bowel disease. *Nat Microbiol*. 2019;4(2):293–305. doi:10.1038/s41564-018-0306-4.
  8. Cekin AH. A microbial signature for Crohn's disease. *Turk J Gastroenterol*. 2017;28(3):237–238. doi:10.5152/tjg.2017.24031.
  9. Halfvarson J, Brislawn CJ, Lamendella R, Vázquez-Baeza Y, Walters WA, Bramer LM, D'Amato M, Bonfiglio F, McDonald D, Gonzalez A. et al. Dynamics of the human gut microbiome in inflammatory bowel disease. *Nat Microbiol*. 2017;2(5):17004. doi:10.1038/nmicrobiol.2017.4.
  10. Correa-Oliveira R, Fachi JL, Vieira A, Sato FT, Vinolo MAR. Regulation of immune cell function by short-chain fatty acids. *Clin Trans Immunol*. 2016;5(4):e73. doi:10.1038/cti.2016.17.
  11. Diederer K, Li JV, Donachie GE, de Meij TG, de Waart DR, Hakvoort TBM, Kindermann A, Wagner J, Auyeung V, Te Velde AA. et al. Exclusive enteral nutrition mediates gut microbial and metabolic changes that are associated with remission in children with crohn's disease. *Sci Rep*. 2020;10(1):18879. doi:10.1038/s41598-020-75306-z.
  12. Kostovcikova K, Coufal S, Galanova N, Fajstova A, Hudcovic T, Kostovcik M, Prochazkova P, Jiraskova Zakostelska Z, Cermakova M, Sediva B. et al. Diet rich in animal protein promotes pro-inflammatory macrophage response and exacerbates colitis in mice. *Front Immunol*. 2019;10:919. doi:10.3389/fimmu.2019.00919.
  13. Fremder M, Kim SW, Khamaysi A, Shimshilashvili L, Eini-Rider H, Park IS, Hadad U, Cheon JH, Ohana E. A transepithelial pathway delivers succinate to macrophages, thus perpetuating their pro-inflammatory metabolic state. *Cell Rep*. 2021;36(6):109521. doi:10.1016/j.celrep.2021.109521.
  14. Tannahill GM, Curtis AM, Adamik J, Palsson-McDermott EM, McGettrick AF, Goel G, Frezza C, Bernard NJ, Kelly B, Foley NH. et al. Succinate is an inflammatory signal that induces IL-1 $\beta$  through HIF-1 $\alpha$ . *Nature*. 2013;496(7444):238–242. doi:10.1038/nature11986.
  15. Macias-Ceja DC, Ortiz-Masia D, Salvador P, Gisbert-Ferrández L, Hernández C, Hausmann M, Rogler G, Esplugues JV, Hinojosa J, Alós R. et al. Succinate receptor mediates intestinal inflammation and fibrosis. *Mucosal Immunol*. 2019;12(1):178–187. doi:10.1038/s41385-018-0087-3.
  16. Yan XL, Liu XC, Zhang YN, Du TT, Ai Q, Gao X, Yang JL, Bao L, Li LQ. Succinate aggravates intestinal injury in mice with necrotizing enterocolitis. *Front Cell Infect Microbiol*. 2022;12:1064462. doi:10.3389/fcimb.2022.1064462.
  17. Connors J, Dawe N, Van Limbergen J. The role of succinate in the regulation of intestinal inflammation. *Nutrients*. 2018;11(1):11. doi:10.3390/nu11010025.
  18. Harrison OJ, Srinivasan N, Pott J, Schiering C, Krausgruber T, Ilott NE, Maloy KJ. Epithelial-derived IL-18 regulates Th17 cell differentiation and Foxp3(+) Treg cell function in the intestine. *Mucosal Immunol*. 2015;8(6):1226–1236. doi:10.1038/mi.2015.13.
  19. Munoz M, Eidenschenk C, Ota N, Wong K, Lohmann U, Kühl AA, Wang X, Manzanillo P, Li Y, Rutz S. et al. Interleukin-22 induces interleukin-18 expression from epithelial cells during intestinal infection. *Immunity*. 2015;42(2):321–331. doi:10.1016/j.immuni.2015.01.011.
  20. Chiang HY, Lu HH, Sudhakar JN, Chen Y-W, Shih N-S, Weng Y-T, Shui J-W. IL-22 initiates an IL-18-dependent epithelial response circuit to enforce intestinal host defence. *Nat Commun*. 2022;13(1):874. doi:10.1038/s41467-022-28478-3.
  21. Iljazovic A, Roy U, Galvez EJC, Lesker TR, Zhao B, Gronow A, Amend L, Will SE, Hofmann JD, Pils MC. et al. Perturbation of the gut microbiome by *Prevotella* spp. enhances host susceptibility to mucosal inflammation. *Mucosal Immunol*. 2021;14(1):113–124. doi:10.1038/s41385-020-0296-4.
  22. Levy M, Thaïs CA, Zeevi D, Dohnalová L, Zilberman-Schapira G, Mahdi J, David E, Savidor A, Korem T, Herzig Y. et al. Microbiota-modulated metabolites shape the intestinal microenvironment by regulating NLRP6 inflammasome signaling. *Cell*. 2015;163(6):1428–1443. doi:10.1016/j.cell.2015.10.048.
  23. Pu Z, Che Y, Zhang W, Sun H, Meng T, Xie H, Cao L, Hao H. Dual roles of IL-18 in colitis through regulation of the function and quantity of goblet cells. *Int J Mol Med*. 2019;43:2291–2302. doi:10.3892/ijmm.2019.4156.
  24. Nowarski R, Jackson R, Gagliani N, de Zoete M, Palm N, Bailis W, Low J, Harman CD, Graham M,



- Elinav E. et al. Epithelial IL-18 equilibrium controls barrier function in colitis. *Cell*. 2015;163(6):1444–1456. doi:10.1016/j.cell.2015.10.072.
25. Chassaing B, Aitken JD, Malleshappa M, Vijay-Kumar M. Dextran sulfate sodium (DSS)-induced colitis in mice. *Curr Protoc Immunol*. 2014;104(1):15–25. doi:10.1002/0471142735.im1525s104.
26. Chassaing B, Srinivasan G, Delgado MA, Young AN, Gewirtz AT, Vijay-Kumar M. Fecal lipocalin 2, a sensitive and broadly dynamic non-invasive biomarker for intestinal inflammation. *PLOS ONE*. 2012;7(9):e44328. doi:10.1371/journal.pone.0044328.
27. Firpo MA, Rollins MD, Szabo A, Gull JD, Jackson JD, Shao Y, Glasgow RE, Mulvihill SJ. A conscious mouse model of gastric ileus using clinically relevant endpoints. *BMC Gastroenterol*. 2005;5(1):18. doi:10.1186/1471-230X-5-18.
28. Roy U, Galvez EJC, Iljazovic A, Lesker TR, Błażejowski AJ, Pils MC, Heise U, Huber S, Flavell RA, Strowig T. et al. Distinct microbial communities trigger colitis development upon intestinal barrier damage via innate or adaptive immune cells. *Cell Rep*. 2017;21(4):994–1008. doi:10.1016/j.celrep.2017.09.097.
29. Bloom SM, Bijanki VN, Nava GM, Sun L, Malvin N, Donermeyer D, Dunne W, Allen P, Stappenbeck T. Commensal bacteroides species induce colitis in host-genotype-specific fashion in a mouse model of inflammatory bowel disease. *Cell Host Microbe*. 2011;9(5):390–403. doi:10.1016/j.chom.2011.04.009.
30. Li X, Ren Y, Zhang J, Ouyang C, Wang C, Lu F, Yin Y. Development of early-life gastrointestinal microbiota in the presence of antibiotics alters the severity of acute DSS-Induced colitis in mice. *Microbiol Spectr*. 2022;10(3):e0269221. doi:10.1128/spectrum.02692-21.
31. Huang C, Tan H, Song M, Liu K, Liu H, Wang J, Shi Y, Hou F, Zhou Q, Huang R. et al. Maternal Western diet mediates susceptibility of offspring to crohn's-like colitis by deoxycholate generation. *Microbiome*. 2023;11(1):96. doi:10.1186/s40168-023-01546-6.
32. Van der Meulen R, Adriany T, Verbrugghe K, De Vuyst L. Kinetic analysis of bifidobacterial metabolism reveals a minor role for succinic acid in the regeneration of NAD<sup>+</sup> through its growth-associated production. *Appl Environ Microbiol*. 2006;72(8):5204–5210. doi:10.1128/AEM.00146-06.
33. Leibovitz H, Lee SH, Xue M, Garay JA, Hernandez-Rocha C, Madsen KL, Meddings JB, Guttman DS, Espin-Garcia O, Smith MI. et al. Altered gut microbiome composition and function are associated with gut barrier dysfunction in healthy relatives of patients with Crohn's disease. *Gastroenterology*. 2022;163(5):1364–1376 e10. doi:10.1053/j.gastro.2022.07.004.
34. Zhu S, Han M, Liu S, Fan L, Shi H, Li P. Composition and diverse differences of intestinal microbiota in ulcerative colitis patients. *Front Cell Infect Microbiol*. 2022;12:953962. doi:10.3389/fcimb.2022.953962.
35. XX H, YH L, PG Y, Meng X-C, Chen C-Y, Li K-M, Li J-N. Relationship between clinical features and intestinal microbiota in Chinese patients with ulcerative colitis. *World J Gastroenterol*. 2021;27(28):4722–4737. doi:10.3748/wjg.v27.i28.4722.
36. Lacroix V, Cassard A, Mas E, Barreau F. Multi-omics analysis of gut microbiota in inflammatory bowel diseases: what benefits for diagnostic, prognostic and therapeutic tools? *Int J Mol Sci*. 2021;22(20):22. doi:10.3390/ijms222011255.
37. Vernia P, Caprilli R, Latella G, Barbetti F, Magliocca FM, Cittadini M. Fecal lactate and ulcerative colitis. *Gastroenterology*. 1988;95(6):1564–1568. doi:10.1016/S0016-5085(88)80078-7.
38. Kaczmarczyk O, Dabek-Drobny A, Wozniakiewicz M, Paśko P, Dobrowolska-Iwanek J, Woźniakiewicz A, Piątek-Guziewicz A, Zagrodzki P, Mach T, Zwolińska-Wcisło M. et al. Fecal levels of lactic, succinic and short-chain fatty acids in patients with ulcerative colitis and Crohn disease: a pilot study. *J Clin Med*. 2021;10(20):10. doi:10.3390/jcm10204701.
39. Bauset C, Lis-Lopez L, Coll S, Gisbert-Ferrándiz L, Macias-Ceja DC, Seco-Cervera M, Navarro F, Esplugues JV, Calatayud S, Ortiz-Masia D. et al. SUCNR1 mediates the priming step of the inflammatory in intestinal epithelial cells: relevance in ulcerative colitis. *Biomedicines*. 2022;10(3):10. doi:10.3390/biomedicines10030532.
40. Dudley EG, Steele JL. Succinate production and citrate catabolism by Cheddar cheese nonstarter lactobacilli. *J Appl Microbiol*. 2005;98(1):14–23. doi:10.1111/j.1365-2672.2004.02440.x.
41. Kaneuchi C, Seki M, Komagata K. Production of succinic acid from citric acid and related acids by lactobacillus strains. *Appl Environ Microbiol*. 1988;54(12):3053–3056. doi:10.1128/aem.54.12.3053-3056.1988.
42. Monfort-Ferre D, Caro A, Menacho M, Martí M, Espina B, Boronat-Toscano A, Nuñez-Roa C, Seco J, Bautista M, Espín E. et al. The gut microbiota metabolite succinate promotes adipose tissue browning in crohn's disease. *J Crohns Colitis*. 2022;16(10):1571–1583. doi:10.1093/ecco-jcc/jjac069.
43. Louis P, Flint HJ. Formation of propionate and butyrate by the human colonic microbiota. *Environ Microbiol*. 2017;19(1):29–41. doi:10.1111/1462-2920.13589.
44. Watanabe Y, Nagai F, Morotomi M. Characterization of *Phascolarctobacterium succinatutens* sp. nov. an asaccharolytic, succinate-utilizing bacterium isolated from human feces. *Appl Environ Microbiol*. 2012;78(2):511–518. doi:10.1128/AEM.06035-11.
45. Grill JI, Neumann J, Hiltwein F, Kolligs FT, Schneider MR. Intestinal E-cadherin deficiency aggravates dextran sodium sulfate-induced colitis. *Dig Dis Sci*. 2015;60(4):895–902. doi:10.1007/s10620-015-3551-x.
46. Kuo WT, Zuo L, Odenwald MA, Madha S, Singh G, Gurniak CB, Abraham C, Turner JR. The tight junction protein ZO-1 is dispensable for barrier function but

- critical for effective mucosal repair. *Gastroenterology*. 2021;161(6):1924–1939. doi:10.1053/j.gastro.2021.08.047.
47. Ahmad R, Kumar B, Thapa I, Tamang RL, Yadav SK, Washington MK, Talmon GA, Yu AS, Bastola DK, Dhawan P. et al. Claudin-2 protects against colitis-associated cancer by promoting colitis-associated mucosal healing. *J Clin Invest*. 2023;133(23). doi:10.1172/JCI1170771.
  48. Weiss ES, Girard-Guyonvarc'h C, Holzinger D, de Jesus AA, Tariq Z, Picarsic J, Schiffrin EJ, Foell D, Grom AA, Ammann S. et al. Interleukin-18 diagnostically distinguishes and pathogenically promotes human and murine macrophage activation syndrome. *Blood*. 2018;131(13):1442–1455. doi:10.1182/blood-2017-12-820852.
  49. Zaki MH, Vogel P, Body-Malapel M, Lamkanfi M, Kanneganti T-D. IL-18 production downstream of the Nlrp3 inflammasome confers protection against colorectal tumor formation. *J Immunol*. 2010;185(8):4912–4920. doi:10.4049/jimmunol.1002046.
  50. Armstrong H, Mander I, Zhang Z, Armstrong D, Wine E. Not all fibers are born equal; variable response to dietary fiber subtypes in IBD. *Front Pediatr*. 2020;8:620189. doi:10.3389/fped.2020.620189.
  51. Desai MS, Seekatz AM, Koropatkin NM, Kamada N, Hickey CA, Wolter M, Pudlo NA, Kitamoto S, Terrapon N, Muller A. et al. A dietary fiber-deprived gut microbiota degrades the colonic mucus barrier and enhances pathogen susceptibility. *Cell*. 2016;167(5):1339–1353 e21. doi:10.1016/j.cell.2016.10.043.
  52. Armstrong HK, Bording-Jorgensen M, Santer DM, Zhang Z, Valcheva R, Rieger AM, Kim JS, Dijk SI, Mahmood R, Ogungbola O. et al. Unfermented  $\beta$ -fructan fibers fuel inflammation in select inflammatory bowel disease patients. *Gastroenterology*. 2023;164(2):228–240. doi:10.1053/j.gastro.2022.09.034.
  53. Singh V, Yeoh BS, Walker RE, Xiao X, Saha P, Golonka RM, Cai J, Bretin ACA, Cheng X, Liu Q. et al. Microbiota fermentation-NLRP3 axis shapes the impact of dietary fibres on intestinal inflammation. *Gut*. 2019;68(10):1801–1812. doi:10.1136/gutjnl-2018-316250.
  54. Gearry RB, Irving PM, Barrett JS, Nathan DM, Shepherd SJ, Gibson PR. Reduction of dietary poorly absorbed short-chain carbohydrates (FODMAPs) improves abdominal symptoms in patients with inflammatory bowel disease—a pilot study. *J Crohns Colitis*. 2009;3(1):8–14. doi:10.1016/j.crohns.2008.09.004.
  55. Prince AC, Myers CE, Joyce T, Irving P, Lomer M, Whelan K. Fermentable carbohydrate restriction (low FODMAP diet) in clinical practice improves functional gastrointestinal symptoms in patients with inflammatory bowel disease. *Inflamm Bowel Dis*. 2016;22(5):1129–1136. doi:10.1097/MIB.0000000000000708.
  56. Maagaard L, Ankersen DV, Vegh Z, Burisch J, Jensen L, Pedersen N, Munkholm P. Follow-up of patients with functional bowel symptoms treated with a low FODMAP diet. *World J Gastroenterol*. 2016;22(15):4009–4019. doi:10.3748/wjg.v22.i15.4009.
  57. Kaplan GG, Ng SC. Understanding and preventing the global increase of inflammatory bowel disease. *Gastroenterology*. 2017;152(2):313–321 e2. doi:10.1053/j.gastro.2016.10.020.
  58. Peters V, Dijkstra G, Campmans-Kuijpers MJE. Are all dietary fibers equal for patients with inflammatory bowel disease? A systematic review of randomized controlled trials. *Nutr Rev*. 2022;80(5):1179–1193. doi:10.1093/nutrit/nuab062.
  59. Hernandez-Chirilaque C, Aranda CJ, Ocon B, Capitán-Cañadas F, Ortega-González M, Carrero JJ, Suárez MD, Zarzuelo A, Sánchez de Medina F, Martínez-Augustin O. et al. Germ-free and antibiotic-treated mice are highly susceptible to epithelial injury in DSS colitis. *J Crohns Colitis*. 2016;10(11):1324–1335. doi:10.1093/ecco-jcc/jjw096.
  60. Dai ZF, Ma XY, Yang RL, Wang H, Xu D, Yang J, Guo X, Meng S, Xu R, Li Y. et al. Intestinal flora alterations in patients with ulcerative colitis and their association with inflammation. *Exp Ther Med*. 2021;22(5):1322. doi:10.3892/etm.2021.10757.
  61. Guo W, Mao B, Cui S, Tang X, Zhang Q, Zhao J, Zhang H. Protective effects of a novel probiotic bifidobacterium pseudolongum on the intestinal barrier of colitis mice via modulating the Ppar $\gamma$ /STAT3 pathway and intestinal microbiota. *Foods*. 2022;11(11):1551. doi:10.3390/foods11111551.
  62. Wang W, Chen L, Zhou R, Wang X, Song L, Huang S, Wang G, Xia B. Increased proportions of Bifidobacterium and the Lactobacillus group and loss of butyrate-producing bacteria in inflammatory bowel disease. *J Clin Microbiol*. 2014;52(2):398–406. doi:10.1128/JCM.01500-13.
  63. Wang SP, Rubio LA, Duncan SH, Donachie GE, Holtrop G, Lo G, Farquharson FM, Wagner J, Parkhill J, Louis P. et al. Pivotal roles for pH, lactate, and lactate-utilizing bacteria in the stability of a human colonic microbial ecosystem. *mSystems*. 2020;5(5). doi:10.1128/mSystems.00645-20.
  64. Bourriaud C, Robins RJ, Martin L, Kozłowski F, Tenailleau E, Cherbut C, Michel C. Lactate is mainly fermented to butyrate by human intestinal microfloras but inter-individual variation is evident. *J Appl Microbiol*. 2005;99(1):201–212. doi:10.1111/j.1365-2672.2005.02605.x.
  65. Weghoff MC, Bertsch J, Muller V. A novel mode of lactate metabolism in strictly anaerobic bacteria. *Environ Microbiol*. 2015;17(3):670–677. doi:10.1111/1462-2920.12493.
  66. Reichardt N, Duncan SH, Young P, Belenguer A, McWilliam Leitch C, Scott KP, Flint HJ, Louis P. Phylogenetic distribution of three pathways for propionate production within the human gut microbiota. *Isme J*. 2014;8(6):1323–1335. doi:10.1038/ismej.2014.14.

67. Culp EJ, Goodman AL. Cross-feeding in the gut microbiome: ecology and mechanisms. *Cell Host Microbe*. 2023;31(4):485–499. doi:10.1016/j.chom.2023.03.016.
68. Littlewood-Evans A, Sarret S, Apfel V, Loesle P, Dawson J, Zhang J, Muller A, Tigani B, Kneuer R, Patel S. et al. GPR91 senses extracellular succinate released from inflammatory macrophages and exacerbates rheumatoid arthritis. *J Exp Med*. 2016;213(9):1655–1662. doi:10.1084/jem.20160061.
69. Hove H, Mortensen PB. Influence of intestinal inflammation (IBD) and small and large bowel length on fecal short-chain fatty acids and lactate. *Dig Dis Sci*. 1995;40(6):1372–1380. doi:10.1007/BF02065554.
70. He L, Wang H, Zhang Y, Geng L, Yang M, Xu Z, Zou K, Xu W, Gong S. Evaluation of monocarboxylate transporter 4 in inflammatory bowel disease and its potential use as a diagnostic marker. *Dis Markers*. 2018;2018:1–6. doi:10.1155/2018/2649491.
71. Taylor SJ, Winter MG, Gillis CC, Silva LAD, Dobbins AL, Muramatsu MK, Jimenez AG, Chanin RB, Spiga L, Llano EM. et al. Colonocyte-derived lactate promotes *E. coli* fitness in the context of inflammation-associated gut microbiota dysbiosis. *Microbiome*. 2022;10(1):200. doi:10.1186/s40168-022-01389-7.
72. Song Y, Xie F, Ma S, Deng G, Li Y, Nie Y, Wang F, Yu G, Gao Z, Chen K. et al. Caveolin-1 protects against DSS-induced colitis through inhibiting intestinal nitrosative stress and mucosal barrier damage in mice. *Biochem Pharmacol*. 2020;180:114153. doi:10.1016/j.bcp.2020.114153.
73. Garvey EP, Oplinger JA, Furfine ES, Kiff RJ, Laszlo F, Whittle BJR, Knowles RG. 1400W is a slow, tight binding, and highly selective inhibitor of inducible nitric-oxide synthase in vitro and in vivo. *J Biol Chem*. 1997;272(8):4959–4963. doi:10.1074/jbc.272.8.4959.
74. Narula N, Wong ECL, Dehghan M, Mente A, Rangarajan S, Lanas F, Lopez-Jaramillo P, Rohatgi P, Lakshmi PV, Varma RP. et al. Association of ultra-processed food intake with risk of inflammatory bowel disease: prospective cohort study. *BMJ*. 2021;374(1554):1–11. doi:10.1136/bmj.n1554.
75. Chen J, Wellens J, Kalla R, Fu T, Deng M, Zhang H, Yuan S, Wang X, Theodoratou E, Li X. et al. Intake of ultra-processed foods is associated with an increased risk of crohn's disease: a cross-sectional and prospective analysis of 187 154 participants in the UK biobank. *J Crohns Colitis*. 2023;17(4):535–552. doi:10.1093/ecco-jcc/jjac167.
76. Seregin SS, Golovchenko N, Schaf B, Chen J, Pudlo NA, Mitchell J, Baxter NT, Zhao L, Schloss PD, Martens EC. et al. NLRP6 protects Il10 (-/-) mice from colitis by limiting colonization of Akkermansia muciniphila. *Cell Rep*. 2017;19(10):2174. doi:10.1016/j.celrep.2017.05.074.
77. Deol P, Ruegger P, Logan GD, Shawki A, Li J, Mitchell JD, Yu J, Piamthai V, Radi SH, Hasnain S. et al. Diet high in linoleic acid dysregulates the intestinal endocannabinoid system and increases susceptibility to colitis in mice. *Gut Microbes*. 2023;15(1):2229945. doi:10.1080/19490976.2023.2229945.
78. Montbarbon M, Pichavant M, Langlois A, Erdual E, Maggioro F, Neut C, Mallevaey T, Dharancy S, Dubuquoy L, Trottein F. et al. Colonic inflammation in mice is improved by cigarette smoke through iNKT cells recruitment. *PLOS ONE*. 2013;8(4):e62208. doi:10.1371/journal.pone.0062208.
79. Singh V, Kumar M, San Yeoh B, Xiao X, Saha P, Kennett MJ, Vijay-Kumar M. Inhibition of interleukin-10 signaling induces microbiota-dependent chronic colitis in apolipoprotein E deficient mice. *Inflamm Bowel Dis*. 2016;22(4):841–852. doi:10.1097/MIB.0000000000000699.
80. Lei W, Ren W, Ohmoto M, Urban JF, Matsumoto I, Margolskee RF, Jiang P. Activation of intestinal tuft cell-expressed *Sucnr1* triggers type 2 immunity in the mouse small intestine. *Proc Natl Acad Sci USA*. 2018;115(21):5552–5557. doi:10.1073/pnas.1720758115.
81. Tsuru A, Fujimoto N, Takahashi S, Saito M, Nakamura D, Iwano M, Iwawaki T, Kadokura H, Ron D, Kohno K. Negative feedback by IRE1 $\beta$  optimizes mucin production in goblet cells. *Proc Natl Acad Sci U S A*. 2013;110(8):2864–2869. doi:10.1073/pnas.1212484110.
82. Zwanziger D, Rakov H, Engels K, Moeller LC, Führer D. Sex-dependent claudin-1 expression in the liver of euthyroid and hypothyroid mice. *Eur Thyroid J*. 2015;4(1):67–73. doi:10.1159/000431316.
83. Zou J, Chassaing B, Singh V, Pellizzon M, Ricci M, Fythe MD, Kumar MV, Gewirtz AT. Fiber-mediated nourishment of gut microbiota protects against diet-induced obesity by restoring IL-22-mediated colonic health. *Cell Host Microbe*. 2018;23(1):41–53 e4. doi:10.1016/j.chom.2017.11.003.
84. Su H, Xie L, Xu Y, Ke H, Bao T, Li Y, Chen W. Pelargonidin-3-O-glucoside derived from wild raspberry exerts antihyperglycemic effect by inducing autophagy and modulating gut microbiota. *J Agric Food Chem*. 2020;68(46):13025–13037. doi:10.1021/acs.jafc.9b03338.
85. Holmes JL, Van Itallie CM, Rasmussen JE, Anderson JM. Claudin profiling in the mouse during postnatal intestinal development and along the gastrointestinal tract reveals complex expression patterns. *Gene Expr Patterns*. 2006;6(6):581–588. doi:10.1016/j.modgep.2005.12.001.
86. Van den Bossche J, Laoui D, Morias Y, Movahedi K, Raes G, De Baetselier P, Van Genderachter JA. Claudin-1, claudin-2 and claudin-11 genes differentially associate with distinct types of anti-inflammatory macrophages in vitro and with parasite- and tumour-elicited

- macrophages in vivo. *Scand J Immunol.* **2012**;75(6):588–598. doi:[10.1111/j.1365-3083.2012.02689.x](https://doi.org/10.1111/j.1365-3083.2012.02689.x).
87. Fernandez-Martin JC, Espinosa-Oliva AM, Garcia-Dominguez I, Rosado-Sánchez I, Pacheco YM, Moyano R, Monterde JG, Venero JL, de Pablos RM. Gal3 plays a deleterious role in a mouse model of endotoxemia. *Int J Mol Sci.* **2022**;23(3):23. doi:[10.3390/ijms23031170](https://doi.org/10.3390/ijms23031170).
  88. Tsuboi K, Nishitani M, Takakura A, Imai Y, Komatsu M, Kawashima H. Autophagy protects against colitis by the maintenance of normal gut microflora and secretion of mucus. *J Biol Chem.* **2015**;290(33):20511–20526. doi:[10.1074/jbc.M114.632257](https://doi.org/10.1074/jbc.M114.632257).
  89. Sakazaki Y, Hoshino T, Takei S, Sawada M, Oda H, Takenaka S-I, Imaoka H, Matsunaga K, Ota T, Abe Y. et al. Overexpression of chitinase 3-like 1/YKL-40 in lung-specific IL-18-transgenic mice, smokers and COPD. *PLOS ONE.* **2011**;6(9):e24177. doi:[10.1371/journal.pone.0024177](https://doi.org/10.1371/journal.pone.0024177).
  90. Katakura K, Lee J, Rachmilewitz D, Li G, Eckmann L, Raz E. Toll-like receptor 9-induced type I IFN protects mice from experimental colitis. *J Clin Invest.* **2005**;115(3):695–702. doi:[10.1172/JCI22996](https://doi.org/10.1172/JCI22996).
  91. Tian S, Paudel D, Hao F, Neupane R, Castro R, Patterson AD, Tiwari AK, Prabhu KS, Singh V. Refined fiber inulin promotes inflammation-associated colon tumorigenesis by modulating microbial succinate production. *Cancer Rep (Hoboken).* **2023**;6(11):e1863. doi:[10.1002/cnr2.1863](https://doi.org/10.1002/cnr2.1863).
  92. Singh V, Yeoh BS, Abokor AA, Golonka RM, Tian Y, Patterson AD, Joe B, Heikenwalder M, Vijay-Kumar M. Vancomycin prevents fermentable fiber-induced liver cancer in mice with dysbiotic gut microbiota. *Gut Microbes.* **2020**;11(4):1077–1091. doi:[10.1080/19490976.2020.1743492](https://doi.org/10.1080/19490976.2020.1743492).
  93. Singh V, Chassaing B, Zhang L, San Yeoh B, Xiao X, Kumar M, Baker M, Cai J, Walker R, Borkowski K. et al. Microbiota-dependent hepatic lipogenesis mediated by Stearoyl CoA Desaturase 1 (SCD1) promotes metabolic syndrome in TLR5-deficient mice. *Cell Metab.* **2015**;22(6):983–996. doi:[10.1016/j.cmet.2015.09.028](https://doi.org/10.1016/j.cmet.2015.09.028).
  94. Singh V, Yeoh BS, Chassaing B, Xiao X, Saha P, Aguilera Olvera R, Lapek JD, Zhang L, Wang W-B, Hao S. et al. Dysregulated microbial fermentation of soluble fiber induces cholestatic liver cancer. *Cell.* **2018**;175(3):679–694 e22. doi:[10.1016/j.cell.2018.09.004](https://doi.org/10.1016/j.cell.2018.09.004).
  95. Caporaso JG, Lauber CL, Walters WA, Berg-Lyons D, Huntley J, Fierer N, Owens SM, Betley J, Fraser L, Bauer M. et al. Ultra-high-throughput microbial community analysis on the illumina HiSeq and MiSeq platforms. *Isme J.* **2012**;6(8):1621–1624. doi:[10.1038/ismej.2012.8](https://doi.org/10.1038/ismej.2012.8).
  96. Bolyen E, Rideout JR, Dillon MR, Bokulich NA, Abnet CC, Al-Ghalith GA, Alexander H, Alm EJ, Arumugam M, Asnicar F. et al. Reproducible, interactive, scalable and extensible microbiome data science using QIIME 2. *Nat Biotechnol.* **2019**;37(8):852–857. doi:[10.1038/s41587-019-0209-9](https://doi.org/10.1038/s41587-019-0209-9).
  97. Callahan BJ, McMurdie PJ, Rosen MJ, Han AW, Johnson AJA, Holmes SP. DADA2: high-resolution sample inference from illumina amplicon data. *Nat Methods.* **2016**;13(7):581–583. doi:[10.1038/nmeth.3869](https://doi.org/10.1038/nmeth.3869).
  98. Mallick H, Rahnavard A, McIver LJ, Ma S, Zhang Y, Nguyen LH, Tickle TL, Weingart G, Ren B, Schwager EH. et al. Multivariable association discovery in population-scale meta-omics studies. *PLoS Comput Biol.* **2021**;17(11):e1009442. doi:[10.1371/journal.pcbi.1009442](https://doi.org/10.1371/journal.pcbi.1009442).